Arkadia degrades SNON to activate level-specific NODAL responses

Jon M. Carthy[1], Marilia Ioannou[1] and Vasso Episkopou[1]*
Department of Medicine, Division of Brain Sciences, Imperial College London
[1]These authors contributed equally to this work
*email: vasso.episkopou@imperial.ac.uk

SUMMARY

NODAL, a transforming-growth-factor-beta (TGF-β)-family ligand, exhibits morphogen functions during gastrulation via its activated transcriptional effectors, SMAD2/3. High signalling-levels specify cell-fates inducing anterior/head, lower specify posterior, and absence abolishes gastrulation. How cells assess NODAL-signalling levels to initiate specific gene expression patterns remains elusive.

Here, we show that the co-repressor SNON represses a subset of NODAL-SMAD2/3 target-genes and that the activation of these genes depends on SNON removal by the E3-ubiquitin-ligase Arkadia (RNF111). As Arkadia degrades SNON in complex with SMAD2/3, high NODAL-SMAD2/3 signalling is required to saturate SNON and remove it allowing the activation of SNON-repressed targets. *Arkadia-null* embryos lack anterior/head and are rescued by removal of SNON, confirming that SNON represses anterior development which requires also high NODAL-signalling.

Therefore, cells assess NODAL-signalling levels by pairing SMAD2/3 to SNON triggering their degradation by Arkadia. Only high signalling removes SNON that leads to derepression of the SNON-repressed SMAD2/3-targets achieving level specific responses.

INTRODUCTION

SMAD2 and SMAD3 (SMAD2/3) are transcription factors responsible for the responses and numerous functions downstream of the class of TGFβ-family ligands that includes NODAL, Activin-A (Activin) and TGFβ. They are also the signal transducers, because they are phosphorylated at the C-terminus by ligand-activated receptors. Phosphorylated SMAD2/3 (hereafter referred to as SMAD2/3) form complexes with SMAD4 to translocate to the nucleus where they bind to SMAD-binding elements (SBE) on the DNA and recruit transcriptional co-activators to initiate

transcription [1-4]. However, SMAD2/3 and SMAD4 can also recruit co-repressors, SKI and SNON (SKIL), which bring histone deacetylases and silence transcription[5]. Target-gene specificity of SMAD2/3 is regulated by interaction with other transcription partner-factors present in the cell[3,6]. Furthermore, as NODAL is a morphogen, it elicits unique functions and induces specific cell-fates in embryonic cells depend on signalling level[7]. This suggests that SMAD2/3 effectors select different target genes for activation depending on their concentration[7]. However, how a cell assesses SMAD2/3 signalling levels and initiates a corresponding transcriptional response remains largely unknown.

In vertebrates, during gastrulation NODAL-SMAD2/3 signalling is one of the main pathways responsible for generating the germ layers that contain the precursors of all tissues of the body. NODAL signalling levels are instrumental in patterning these germ layers along the anterior-posterior axis. Loss-of-function experiments in mice and gain-of-function experiments in *Xenopus* and *Zebrafish* show that high levels of NODAL are necessary and sufficient for the induction of anterior cell-fates, while lower levels result in more posterior fates[7,8]. Emerging evidence shows that the interpretation of morphogen levels into specific transcriptional programs and cell fates, depends on signalling dynamics and the interactions of the downstream transcriptional gene networks initiated not only by the morphogen but also by additional signals that the cells receive during their initial differentiation period[9 10 11]. However, for cells to respond differently to various signalling levels, a mechanism is required that assess effector levels, but such mechanisms remain elusive.

In *Drosophila,* affinity of transcription factors for DNA binding elements present in different genes has been shown to regulate transcription in a level-dependent manner[12]. However, despite several efforts, such mechanisms have not been found in vertebrates. Interestingly, in the *Drosophila* wing disc, the TGFβ-family morphogen DPP via its activated SMAD-homologous effector, MAD, uses signalling mediated derepression to regulate level-dependent responses by a derepression mechanism. Specifically, in the absence of signalling, several genes including MAD-targets are repressed by Brinker. Upon signalling, MAD forms complexes with another transcriptional repressor, Schnurri and supresses *Brinker* gene transcription leading to derepression of its targets. MAD-targets require higher MAD levels to both derepress and activate them, than MAD-independent genes that require only derepression[13-15]. This mechanism does not have homologues in vertebrates, and the role of repression and derepression in TGFβ-SMAD morphogen activity has not been studied.

In the mouse, anterior (brain/head) is induced in the ectoderm by tissues that derive from the elongating front of the Primitive Streak (PS) and migrate across and opposite

it to the prospective anterior region of the embryo. Anterior-PS cell fates include the anterior definitive endoderm (ADE), the node - which is a structure forming at the elongating end of PS after ADE migration - and the node-derived mesendoderm (ME), which is a cord-like structure extending out of the node along the midline of the embryo and joining the ADE The ADE and the adjacent ME are responsible for inducing brain/head on the overlying ectoderm[16]. Genetic reduction of NODAL or SMAD2/3 results in anterior/head truncations and loss of midline due to failure to induce the anterior-PS derived tissues ADE and node-ME[7,17]. Furthermore, anterior-PS transplantation to another embryo induces a secondary axis (ADE, node-ME with head and midline) and it is considered to be equivalent to the amphibian Spemann's Organiser suggesting that high NODAL signalling is required for Organiser induction[18].

We previously discovered RNF111 (Arkadia), a RING-domain E3 ubiquitin ligase, and showed it is essential for the formation of anterior-PS cell-fates and that it genetically interacts with NODAL[19 20]. These findings are consistent with the fact that high levels of NODAL are required for anterior development suggesting that Arkadia enhances Nodal signalling[20]. Complementary experiments in *Xenopus* animal-cap assays showed that while ADE and ME induction require injection of high *Nodal* mRNA, this can also be achieved by co-injection of low *Nodal* and *Arkadia* mRNA, suggesting that Arkadia potentiates NODAL signalling[21]. Specifically, injection of Arkadia mRNA into one ventro-vegetal blastomere in *Xenopus* produces Spemann's organiser activity leading to partial axis duplication. This activity is abolished by co-injection of a NODAL antagonist, confirming that Arkadia functions via NODAL signalling[21]. Collectively, the above literature establishes that Arkadia is necessary and sufficient for the establishment of high NODAL-signalling responses in vertebrate development. However, to date, the molecular mechanism of Arkadia's function in the embryo remains elusive.

Biochemical experiments conducted mainly in tumour cell lines showed that Arkadia enhances signalling by mediating the degradation of the inhibitory SMAD7[22] and the nuclear co-repressors SNON and SKI, via the ubiquitin proteasomal pathway[23,24]. Interestingly, Arkadia degrades SNON and SKI only when they are bound to SMAD2/3[23], and experiments in mouse embryos and embryonic stem cells (ESCs) show that it also degrades SMAD2/3[20]. However, whether these substrates mediate the function of Arkadia in the embryo has yet to be determined.

Here we show that genetic removal of *SnoN* but not *Smad7* from *Ark*-/- embryos ([*SnoN/Ark*]-/- rescues anterior-PS derived tissues and restores the midline and anterior/head development, while embryos with individual knock-out of *SnoN* (*SnoN*-

/-) or *Smad7* (*Smad7*-/-) are normal. Similarly, while *Ark*-/- ESCs cannot differentiate towards ADE/ME, [*SnoN/Ark*]-/- ESCs can. Together these data show that Arkadia functions mainly by removing SNON. We have also identified Arkadia-dependent SMAD2/3 targets and show that their expression depends on the removal of SNON by Arkadia. We confirm that Arkadia also degrades SMAD2/3-SNON complexes in embryonic cells and show that SNON is present prior to signalling-induction, consistent with the model that SMAD4-SNON complexes establish repression prior to signalling. Finally, we show that derepression and expression of SNON-repressed targets occurs upon signalling initiation and that high levels of SMAD2/3-signalling are required. This mechanism explains how cells assess levels of NODAL signalling and initiate different transcriptional responses.

Therefore, the mechanism that regulates NODAL level-specific gene-responses shares the same principles with that regulating the *Drosophila* DPP-MAD level specific gene expression[25]. They both involve a transcriptional repressor and a mechanism of derepression, which is regulated by signalling levels. Interestingly, the TGFβ-SMAD2/3 pathway along with SNON and Arkadia are also expressed and operate in adult tissues and are involved in cancer[26-28] suggesting that this mechanism is intrinsic to this pathway and operates broadly.

RESULTS

Arkadia functions via SNON in Embryonic Cells

SNON, SKI and SMAD7 are the substrates of Arkadia within the NODAL/TGFβ pathway. To identify which one mediates its function in embryonic cells we used the Arkadia-dependent SMAD2/3-luciferase reporter (*CAGA*$_{12}$-lucif containing 12 SMAD binding element; SBE)[23] in mouse embryonic fibroblasts (MEFs). This reporter is highly induced by signalling in *Wt* MEFs, but unresponsive in the absence of Arkadia, even with increasing levels of ligand (Extended data Fig. 1a). Using CRISPR/Cas9 we deleted each one of the above substrates in *Ark-/-* MEFs and found that removal of SNON can significantly rescue *luciferase* activity induced by TGFβ ligand (Fig. 1a and Extended data Fig. 1b and c). Expression of exogenous GFP-tagged-Arkadia (*Wt-Ark)* in the parental *Ark-/-* MEF cell-line rescues *CAGA*$_{12}$*-luciferase* activity under ligand treatment (Extended data Fig.1d), confirming that the defect in these cells is due to the loss of Arkadia. We also found that *CAGA*$_{12}$*-luciferase* activity in *SnoN-/-* MEFs is similar to that of *Wt* MEFs (Extended data Fig. 1e), excluding the possibility that the

rescue in [*SnoN/Arkadia]-/-* MEFs is due to over-induction of the reporter in the absence of SNON (compensation). Unlike *SnoN,* deletion of *Smad7* or *Ski* in this *Ark-/-* MEF-line does not rescue reporter activity (Extended data Fig. 2), suggesting that in MEFs SNON is the dominant substrate that Arkadia degrades to allow activation of transcriptional responses (*CAGA$_{12}$-luciferase*) upon signalling stimulation.

We then examined whether SNON is the substrate that mediates the function of Arkadia in ESC-differentiation towards ADE-ME with high levels of Activin-A (AA or Activin). For these experiments we derived *Wt* and *Ark-/-* ESC lines from mouse embryos that carry the ADE-ME reporter transgene *Hex-Gfp* (*Rodriguez et al 2001*). We found that all three *Wt* ESC-lines differentiate towards ADE-ME but all three *Ark-/-* fail to do so (Fig. 1b). However, deletion of *SnoN* in *Ark-/-* ESCs ([*SnoN/Ark*]-/-) using CRISPR/Cas9 (n=10 CRISPR clones generated Extended data Fig 3a) rescues their ability to differentiate towards ADE-ME (Fig 3b). We confirmed the differentiation by western blot analysis with GFP antibody (Extended data Fig. 3b). However, as *Hex-Gfp* is also expressed in the anterior visceral endoderm, which is present in *Ark-/-* embryos[20], we used quantitative PCR (qPCR) for *Cxcr4* definitive endoderm marker[29] and *Foxa2* mesendoderm specific markers[30] and confirmed that the *Hex-Gfp* expression correspond to ADE (Fig 1c). Three *SnoN-/-* ESC lines showed an ability to differentiate towards the ADE (Extended data Fig. 3c and d) excluding the possibility that the rescue of ADE differentiation in [*SnoN/Ark*]-/- is due to an adjustment by excessive ADE differentiation in the absence of SNON. The above data show that Arkadia functions via SNON in ESC-differentiation towards ADE-ME and suggest that SMAD2/3 target genes specifying ADE-ME are repressed by SNON and depend on Arkadia for derepression.

Arkadia functions via SNON in the embryo

To address whether removal of *SnoN* from *Ark-/-* embryos can rescue their phenotype, we used mice, *Skil^{tm2Spw}* (*SnoN-/-*)[31]. *Skil^{tm2Spw}* homozygous mice are viable and fertile. Therefore, to eliminate any doubts as to whether this mutation has successfully disrupted the *SnoN* gene, we performed whole mount *in situ* hybridization (WISH) at embryonic day 8.5 (E8.5) embryos and confirmed that homozygous *Skil^{tm2Spw}* embryos are indeed *SnoN-/-* (Extended Data Fig. 4a-c). We examined the development of ADE in these *SnoN-/-* embryos and found no significant difference in size or timing of development (Extended Data Fig. 4d). The absence of an embryonic phenotype in *SnoN-/-* mice is puzzling, however, we found that the co-repressor SKI, which is the

close homologue of SNON is upregulated in *SnoN*-/- mice (Fig. 1d). SKI, like SNON forms complexes with SMAD2/3, which are recognised and targeted for degradation by Arkadia. It is therefore likely that the above observed upregulation of SKI restores SMAD2/3-signalling repression in the absence of SNON in the embryo.

We found that [*SnoN/Ark*]-/- embryos (n>18) exhibit rescue of ADE, node-ME, and development along with midline and brain/head formation. This remarkable rescue was highly penetrant and consistent in a genetic background greater than six generations backcrossed to 129Sv/Ev (Extended data Fig. 4e).

We assessed ADE development by whole mount *in situ* hybridization (WISH) of embryos stage day E7.5 with *Cerberus (Cerbl)*[32] and found that while *Ark*-/- embryos lack ADE, [*SnoN/Ark*]-/- develop ADE comparable to *Wt* and *SnoN*-/- (Fig. 2a). We then examined the ability of the recovered ADE in *[SnoN/Ark]-/-* to induce forebrain using the forebrain marker *Six3*[33]. E8.5 [*SnoN/Ark*]-/- embryos exhibit obvious head-folds that express *Six3* comparable to *Wt* and *SnoN-/-* embryos (Fig. 2b). We also examined the recovery of node and ME formation in *[SnoN/Ark]-/-* embryos with the specific markers *FoxA2*[30] (Fig. 2c) and *Shh*[34] (Fig. 2d) at stage E8.5 and E9.5 embryos respectively. Both markers confirmed rescue of node and midline development in *[SnoN/Ark]-/-* embryos. However, *[SnoN/Ark]-/-* pups are not born indicating that embryonic development is arrested later on. This may be due to Arkadia and SNON NODAL-independent functions at later embryonic stages. Furthermore, the significant rescue observed during gastrulation by SNON removal from *Ark*-/- embryos suggests that SKI contributes minor repression to SMAD2/3-signalling within the PS. We found that in *SnoN*-/- embryos the co-repressor SKI is upregulated (Fig. 1d) and this most likely compensates for the lost SNON repression applied to SMAD2/3 signalling responses in the PS and prevents the development of a phenotype. This raises the question, why SKI is not upregulated in [*SnoN/Ark*]-/- embryos like it does in *SnoN-/* embryos, to restore sufficient repression and block the rescue? A possible explanation is that because in [*SnoN/Ark*]-/- embryos, the absence of Arkadia stabilises SKI protein and the accumulated SKI inhibits *Ski* gene upregulation. This hypothesis and the role of SKI in SMAD2/3 repression during gastrulation will be addressed in future experiments.

Arkadia also degrades SMAD7, which functions mainly by mediating the degradation of the TGFβ-signalling receptors[22]. *Smad7*-/- embryos do not exhibit patterning defects and embryos develop normally, with some being born and surviving to adulthood[35]. We also examined the *Smad7*-/- embryos and found no evidence of any gastrulation and patterning defect during early development. We therefore used them

to explore the role of SMAD7 in *Ark*-/- embryos by generating [*Smad7/Ark*]-/- embryos (n=18) in genetic background backcrossed five generations to 129SV/Ev. All (n=18) [*Smad7/Ark*]-/- embryos exhibited a phenotype indistinguishable from that of *Ark-/-* embryos indicating that SMAD7 does not inhibit signalling in the absence of Arkadia (Extended data Fig. 4f).

Collectively the above data confirm that SNON is the dominant factor that Arkadia removes *in vivo* to achieve the development of anterior-PS derived tissues, ADE and node-ME, which are capable of inducing brain/head on the overlaying ectoderm and forming the midline in the embryo. During gastrulation NODAL expression is restricted to the PS and NODAL-SMAD2/3 signalling is essential for gastrulation and for both anterior and posterior PS cell fates. This suggests that only the subset of NODAL-SMAD2/3 targets specifying anterior-PS cell-fates depends on Arkadia. Therefore, the rescue of anterior-PS development by SNON removal from *Ark*-/- embryos suggests SNON represses specifically this subset of NODAL-SMAD2/3 targets required for anterior-PS, but not those for posterior fates.

Arkadia derepresses SNON-repressed genes

The identification of Arkadia-dependent (SnoN-repressed) Nodal-targets using a candidate-gene approach and qPCRs in *Ark*-/- and [*SnoN/Ark*]-/- embryos reflected loss and rescue of tissues that express these genes respectively (Extended data Fig. 5a). We therefore used undifferentiated ESCs to perform biological duplicate RNA-sequencing experiments in two different *Wt* and two *Ark-/-* ESC-lines treated with SB431542 (SB; receptor kinase inhibitor) for 4hours (4h) to turn off signalling followed by Activin-A (AA; a ligand used instead of Nodal) over time. To increase confidence in identifying faithful signalling induction, a time-course experiment with three time points was used for sequencing in each ESC-line: T0, SB; T3, 3h AA; and T6, 6h AA (The RNA-sequencing data have been deposited in NCBI Gene expression Omnibus and are accessible through accession number GSE118005).

Western blot analysis of the ESCs at each time point in which sequencing was performed shows high levels of SNON and SKI in the absence of signalling, followed by their reduction during signalling activation in both *Wt* ESC-lines (Fig. 3a). In contrast, in both *Ark-/-* ESC-lines, SNON and SKI are not degraded during SMAD2/3 activation (Fig. 3a) consistent with previous findings in tumour cell-lines that Arkadia degrades these substrates in the presence of signalling[23,24].

We selected 262 genes with 2-fold induction under Activin treatment in both WT ESC-lines at T3 (Extended data Table1 and heat-map Extended data Fig. 5c). This list includes several SMAD2/3 targets previously identified in ESCs[36] and embryonic teratoma cells[37] providing confidence for the selection. 48 of these genes exhibit greater than 1.5-fold difference in average expression at T3 between *WT* and *Ark-/-* and were considered as Ark-dependent (Extended data Table2). Interestingly, we found that the majority of these genes exhibit lower induction at T6 (Extended data Table2 and Extended data Figure X), most likely due to negative feedback activated over time. This revealed a time-dependent defect, because several Ark-dependent genes at T3 become independent at T6 (Fig. 3b and c and Extended data Fig. 6a). This suggests that the function of Arkadia is restricted to the beginning of signalling-exposure in naïve cells.

We then examined with qPCR the expression of a subset of SMAD2/3-induced genes, which were identified above as Arkadia dependent, in [*SnoN/Ark]-/-* ESC-lines at T0 and T3 conditions and compared this to *Wt* and *Ark*-/-. We found expression rescue in the absence of both Arkadia and SNON (Fig.3b), confirming that Arkadia dependent SMAD2/3-induced genes are repressed by SNON. We excluded the possibility that the rescue in [*SnoN/Ark*]-/- ESCs is caused by over-induction of these SMAD2/3 targets in the absence of SNON in three *SnoN*-/- ESC-lines (Extended data Fig. 5b). Therefore, the above data confirm that a subset of SMAD2/3-induced targets is susceptible to SNON repression and depends on Arkadia to remove SNON leading to derepression and activation.

Notably, SNON and SKI are expressed in the absence of signalling (Fig. 3a), suggesting that SNON- and SKI-SMAD4 complexes are recruited to targets (via SMAD4 binding) and establish silencing. Recent findings show that, prior to signalling, SKI-SMAD4 bind and repress the *RORγt* gene (Zhang et al 2017) and SNON-SMAD4 bind and repress the *SnoN* gene[38], supporting the hypothesis that repression is mediated by SMAD4. Interestingly, derepression of *RORγt* is achieved by TGFβ signalling, but this is not sufficient because IL-6, a SMAD-independent signal, is required for its activation[39]. This suggests that SMAD2/3-signalling results in derepression of several genes that are not activated by its effectors. This is reminiscent of the action of Brinker in *Drosophila*, which suppresses several targets that are otherwise activated by MAD and MAD-independent factors and depend on DPP signalling only for derepression[25]. This suggests that the Arkadia-dependent gene-list includes genes that are derepressed by signalling but are activated by SMAD-independent factors. This is consistent with the observation that several of these

targets are expressed in the absence of signalling at T0 and are upregulated at T3. Therefore, derepression may facilitate the co-regulation and co-operation between NODAL and other signalling pathways such as WNT, BMP, FGF, etc, which are known to be instrumental for gastrulation and patterning in all vertebrates[8]. However, targets that are highly dependent on Arkadia tend to be silent in the absence of signalling, suggesting that chromatin states and the presence of other signals and factors may influence the susceptibility of targets for repression by SNON/SKI (Extended Data Fig. 5c). According to this, the above-identified Arkadia-dependent targets are specific for undifferentiated ESCs and may not be the same as those repressed by SNON in the PS or those required for ADE-ME differentiation in the ESC-derived embryoid bodies treated with Activin.

In summary, the above analysis provides molecular evidence that Arkadia removes SNON in the presence of signalling to derepress and permit the expression of the subset of SMAD2/3-iduced targets that are repressed by SNON. This suggests that in the embryo SNON represses the subset of targets require for anterior-PS development.

Arkadia degrades SMAD2/3-SNON complexes

Interestingly, anterior-PS development and ADE-ME differentiation require not only SNON derepression by Arkadia, but also high levels of Nodal signalling, implying that derepression also requires high levels of signalling. Previous findings support the requirement for signalling in the degradation of SNON/SKI by Arkadia and other ubiquitin ligases[40]. Specifically, it has been shown that Arkadia degrades SNON and SKI only when they interact with SMAD2/3[23], that degradation occurs upon signalling initiation, and that SNON is only transiently reduced[41 42]. However, the above experiments were mostly performed in cancer/transformed cell-lines. Here we investigated how signalling regulate the degradation of SNON/SKI by Arkadia in ESCs and obtained similar findings: that SNON and SKI are present in the absence of signalling; that they are reduced upon signalling-induction; and that this reduction requires Arkadia (Fig. 4a). Furthermore, while reduced levels of SKI remain low over time over time with signalling, SNON reduction is transient and occurs within two to three hours (Fig. 4a). Interestingly, SMAD2/3 is stabilised along with SNON/SKI in *Ark-/-* ESCs (Fig. 3a and Fig. 4a) and *Ark-/-* embryos (Fig. 1d and Extended data Fig. 7b). This is consistent with previous findings showing that Arkadia enhances signalling in ESCs by degrading also SMAD2/3[20]. Together these observations support the idea

that in ESCs and embryos Arkadia degrades the fraction of SMAD2/3 that is complexed with SNON and SKI.

SNON, but not SKI, is a direct target of SMAD2/3 (negative feedback) and is upregulated over time with signalling[43 38]. However, Arkadia is not upregulated by signalling (see RNA-database link) and it is known to be unstable[20], suggesting that its capacity to degrade SMAD2/3-SNON complexes is limited. This is consistent with published data showing that overexpression of Arkadia in *Wt* cells enhances signalling[23]. Furthermore, the transient reduction of SNON can explain the data showing that expression-differences between *Wt* and *Ark-/-* ESCs can be seen at T3 but disappear at T6 for several Arkadia-dependent targets (Fig. 3c).

We also used Proximity Ligation Assays (PLA)[44] in *Wt* and in *Ark-/-* MEFs treated for one hour with TGFβ-ligand to visualise and quantify the SMAD2/3-SMAD4 activation-complexes (Fig. 4b) and the SNON-SMAD2/3 repressed complexes (Fig. 4c). We found the activation complexes in the nucleus are comparable in *Wt* and *Ark-/-* MEFs, indicating equivalent signalling activation (Fig. 4b). This can explain why the expression of the subset of targets that is not repressed by SNON remains unaffected in the absence of Arkadia. However, we found that the SNON-SMAD2/3 complexes accumulate in the absence of Arkadia (Fig. 4c). This confirms that SMAD2/3 saturates SNON, enabling Arkadia to trigger degradation of SNON and possibly also SMAD2/3 in these complexes[20,23].

Together the above data indicate that SMAD2/3-SNON complexes mediate the degradation of SNON by Arkadia in embryonic cells without interfering with the formation of the SMAD2/3-SMAD4 activation complexes and the expression of unrepressed targets. Furthermore, the data confirm that SNON is present in the absence of signalling and most likely forms SMAD4-SNON complexes, which can bind via SMAD4 on SBE containing genes and silence transcription. The transient nature of SNON reduction by Arkadia and SMAD2/3-signalling suggests that derepression of repressed targets is brief and occurs upon signalling initiation.

Deep SNON reduction drives derepression

Each SNON molecule can interact with one SMAD2 or one SMAD3 and, therefore, signalling levels can cause proportionate SNON-reduction in the presence of Arkadia. According to this, high levels of SMAD2/3 are required to remove SNON and derepress all targets. This is consistent with the finding that anterior-PS development requires not only Arkadia but also high levels of NODAL-SMAD2/3 signalling.

To address whether the levels of signalling do indeed drive an equivalent SNON depletion, we assessed SMAD2 and SNON levels downstream of specific levels of signalling in *Wt* ESCs during the first hour upon ligand stimulation. To bypass the endogenous expression of TGFβ ligands in ESCs, we controlled signalling activation at the receptor level. We pretreated cells with SB (receptor kinase inhibitor) for 4hrs and then stimulated signalling for 1hr with set levels of Activin (Fig. 5a) or TGFβ1 (Extended data Fig. 6c), and to achieve specific levels of signalling we manipulated receptor activation by titrating the concentration of the inhibitor SB (0, 10, 2.5, 1.2, 0.6, 0.3μM, Fig. 5a and Extended data Fig. 6c). As the treated ESCs are *Wt*, Arkadia degrades SNON-SMAD2/3 complexes and generates proportionate reduction of SNON levels at each concentration of SB inhibitor (Fig. 5a). Quantification of the bands on western blot showed inverse correlation between SMAD2 and SNON levels at all SB concentrations (Fig. 5b). Furthermore, SMAD2/SNON ratios showed an increase proportionate to the decreasing SB concentration (Fig. 5c). Therefore, the above experiments indicate that in *Wt* ESCs, higher signalling achieves deeper reduction of SNON with Activin/SB or TGFβ/SB conditions.

To address whether the SMAD2/SNON protein ratio correlates with the derepression and expression of known SMAD2/3 targets, we used the same Activin/SB treatment and performed qPCR analysis of representative target genes. This shows that each gene exhibits a distinct response at different SMAD2/SNON protein ratios (compare Fig. 5c and d). Specifically, *Lefty1*[45] and *Lefty2*[46] reach peak-expression without any SB-inhibitor corresponding to the highest SMAD2/SNON ratio (compare Fig. 5d and c). On the other hand, *Smad7* reaches peak expression under 0.6μM and 0.3μM SB-inhibitor corresponding to intermediate SMAD2/SNON ratio (compare Fig. 5d Fig. 5c). The variable dependency of SMAD2/3 target-gene expression on Arkadia seen here (Fig. 5c) agrees with the RNA-sequencing data (Fig. 3b and Extended data Table1; Extended data Fig. 5c and Extended data Fig. 6 and Extended data Fig. 7a) and suggests variable susceptibility to SNON repression for each target. This system is therefore capable of generating graded derepression depending on how susceptible each gene is to SNON repression, leading to graded transcriptional responses (Fig. 5d) downstream of specific levels of SNON reduction.

The transient reduction of SNON, which occurs right at the beginning of ligand stimulation, is noteworthy, explaining that cells assess the signalling levels at “first sight”; interpret levels at “first sight”; and make cell-fate decisions during this brief initial period of derepression. Furthermore, the negative feedback triggers upregulation of SNON by signalling and probably consolidates the adopted cell-fates by re-

establishing repression. This is important in preventing cells from fate-shifting under continuous signalling.

DISCUSSION

Mechanisms that vertebrate embryonic cells use to assess morphogen signalling levels and initiate level-specific transcriptional responses are largely unknown. Here we describe the operation of such a mechanism downstream of NODAL-SMAD2/3 signalling-responses in mouse embryos and embryonic cells.

Specifically, we show that the co-repressor SNON, and possibly SKI, repress a subset of NODAL-SMAD2/3 targets (Fig. 3); and that the expression of these repressed targets depends on complex formation of SMAD2/3-SNON upon signalling initiation and that these complexes enable Arkadia to degrade SNON (Fig. 3 and 4). Furthermore, we show that the levels of SMAD2/3 correlate directly with the levels of SNON reduction, along with the derepression and activation of the repressed targets (Fig. 5a-d). We confirmed this mechanism *in vivo,* by showing that removal of SNON from *Ark*-/- embryos or ESCs rescues anterior-PS cell-fate and head formation, or ADE differentiation respectively (Fig. 1 and 2). A model of this mechanism is presented in Fig. 5e.

This mechanism is based on “signalling induced derepression” and shares principles with the regulation of DPP-MAD level-specific functions in *Drosophila*. These similarities suggest that other signalling pathways that exhibit level-specific functions could be using “signalling mediated derepression”.

Interestingly, Arkadia, SNON and SKI are broadly expressed and are also involved in TGFβ-signalling associated tumourigenesis[27] and metastasis[26,28], suggesting that this mechanism is not restricted to embryonic development but operates also in adult cells and tissues. Furthermore, additional E3 ubiquitin ligases have been shown to degrade SNON/SKI in response to signalling in other cells[5], implying that “signalling induced derepression” is intrinsic to the TGFβ-SMAD2/3 pathway and provides functional versatility.

ACKNOWLEDGMENTS

This research has been funded by the MRC UK grant (MR/M011194). We wish to thank Susumu Itoh for donating the Smad7 KO mice and Kunxin Luo (U.C.Berkeley) for the SnoN KO mice. We thank Vikas Sharma, Michael Normal and Nabiha Husain for

preliminary data. Tristan Rodriguez and Aida DiGregorio (ICL) for help with in situ hybridiations, Eleni Ioannou and Zoe Webster (MRC LMS) for technical assistance and animal procedures. We also thank Robin Lovell-Badge (Crick Institute) and Sohaila Rastan for critical reading and advice on the manuscript; and Paul Matthews (ICL) for encouragement and support through difficult times.

METHODS

Mice and Embryo methods

Mice were backcrossed >5 generations to 129Sv/Ev background before they were used for WISH, X-gal staining, RNA or protein extraction. Mice were maintained in pathoge free environment under a Home Office licence (Scientific Procedures) Act 1986. *SnoN*-/- (homozygous for the *Skil*^{tm2Spw} allele[31]) mice were kindly donated by Kuxin Luo (Univ. of California Berkeley). *Smad7*-/- mice mice were kindly donated by Susumu Itoh (Showa Pharmaceutical Univ.). *Ark*-/- mice were generated in the laboratory in the past[19]. Mouse genotyping was performed as in the references and by Transnetyx, Inc automatic genotyping.

Whole-mount in situ hybridization (WISH) and X-gal staining was carried out as described[19,20]. SnoN riboprobe was generated in the laboratory by PCR. T7RNA polymerase promoter was introduced at the 5`-end of the primers designed for the gene of interest, enabling direct in vitro transcription of purified PCR fragments. More detailed info about the primers used can be found in the list of primers. For *Shh*, *Six3*, *Cerl*, *Foxa2* probes see references[19,20,47].

QPCR: Total RNA was extracted from individual whole embryos at E 8.5 stage, using RNeasy Micro kit (Qiagen, 74134). cDNA was generated using the iScript reverse transcription supermix (BioRad, 1708840) and QPCR experiments were performed using QuantiFast SYBR Green PCR Kit (Qiagen, 204054), MicroAmp Optical 96 well reaction plates (Applied Biosystems, 4306737) and Stratagene mx3005 qPCR system and software. QPCR experiments were normalised against β-Actin. All p values were determined using one-way ANOVA method (Prism_GraphPad software). Primers/oligonucleotide-sequences used can be found in Extended data Table 2)

Western blots: Total protein extraction was harvested from individual embryos lysed by adding 10 µl of NP-40 buffer (150Mm NaCl, 50mM Tris pH 8, 20mM NaF, 1%NP-40, 1mM EDTA pH 8, plus protease and phosphatase inhibitors). After centrifugation at 100,000 g for 10 min, equal amount of protein extracts was boiled in 2× Laemelli buffer followed by standard SDS-ployacrylamide gel electrophoresis (SDS-PAGE) and transferred onto nitrocellulose membrane. For analysis with antibodies see Cell culture methods.

Cell culture methods

Mouse embryonic fibroblasts (MEFs) were cultured in DMEM containing 10% FBS and supplemented with 1X Penicillin/Streptomycin and L-Gluatamine. Mouse embryonic stem cells were cultured on inactivated MEF feeders and maintained in ES medium containing 15%FBS/DMEM with 1X Pen/Strep and L-Glutamine, 50 uM β-mercaptoethanol and supplemented with additional LIF made in house. Cells were maintained in a humidified incubator at 37 °C and 5% CO2. Prior to performing experiments, cells were maintained in full growth medium supplemented with 10μM SB431542 (Sigma Aldrich, S4317) to inhibit endogenous Smad2/3 signalling. Cells were then washed 2 times in PBS and replaced with medium containing fresh SB431542 or 5ng/mL TGFβ1 (Peprotech, 100-21C) or 10ng/mL Activin A (Sigma Aldrich, A4941) for the indicated time. In certain experiments the concentration of ligand was adjusted; exact experimental conditions are further outlined in the text.

Western blots: Cells were washed once in ice-cold PBS and proteins were collected in lysis buffer (20 mM Tris-HCl pH 8.0, 1% Triton-X, 150 mM NaCl, 2 mM EDTA) supplemented with protease inhibitor cocktail (Roche Diagnostics) and cleared by centrifugation at 12,000x g at 4 °C for 10 min. Equal amounts of protein from each sample were separated by standard SDS-ployacrylamide gel electrophoresis (SDS-PAGE) and transferred to nitrocellulose membrane. Membranes were blocked for 1 h in 5% milk/TBS-T and incubated overnight at 4 °C with primary antibody in TBS-T. Following 3 washes in TBS-T, corresponding HRP-conjugated secondary antibody (Santa Cruz Biotechnology) was added in TBS-T at a concentration of 1:5000 and then incubated for a further 1 h at room temperature. Membranes were washed 3 times in TBS-T and antibody binding was visualised with the enhanced chemiluminescence detection system (Thermo Fischer Scientific Inc.). Images were captured using the GeneGnome XPQ NPC System (Synoptics Limited) and band intensities were calculated. Antibodies used were c-Ski (Santa Cruz Biotechnology, H-329: SC-9140), SnoN (Santa Cruz Biotechnology, H-317: SC-9141), pSmad2 (phosphorylated at Ser465/467 Cell Signaling Technologies: 3101), Smad2/3 (BD Biosciences: 610842); β-Actin (Santa Cruz Biotechnology, SC-47778); β-Tubulin Merck Millipore: (05-661); PCNA (MAB424R).

Proximity Ligation assay (PLA) was performed using the Duolink in situ PLA kit (Sigma) as described[48]. Cells were cultured overnight on 8-well chamber slides, stimulated with TGFβ (or SB43152 control) for the indicated timepoints Primary antibodies were used at a concentration of 1:500 in blocking solution and left overnight

at 4C in a humidified chamber. Dots per nuclei were counted and plotted in bar graphs; each experiment was repeated at least three independent times.

Luciferase assays were performed using the Dual-Luciferase Reporter Assay System (E1910 Promega) according to manufacturer's instructions. MEFs were transiently transfected using Fugene HD with TGF-β/Smad-responsive CAGA12-luc reporter construct and Renilla-Luc plasmid for 24 h prior to stimulation with 5ng/mL TGF-β or 10μM SB43152 for 5 hours. Luciferase activities were measured using a luminometer (GloMax Multi-Detection System, Promega). Normalised promoter activity data are plotted in bar graphs that represent average values from triplicate determinations with standard deviations. Each independent experiment was repeated at least three times.

QPCR were performed as described in mice and embryo methods. Primers sequences are shown in Extended data table 2 and predesigned quantitech primer assays (Qiagen, 249900) were used for other genes including Gal (QT00109970), *RhoB* (QT00249648), Plekha2 (QT00152103), Ncor2 (QT00166439), FoxA2 (QT00242809) and Sox17 (QT00160720). Expression levels of the target genes were quantified by normalizing against β-actin using the delta Ct method.

Embryoid body (EB) differentiation. Mouse *WT* and *Ark*-/- ESCs were trypsinised, and pre-plated on 2% gelatine coated plates for ½ hour to remove feeders, and then transferred to non-coated bacterial dishes at a concentration of 1 X 10^6 cells per 10 cm dish in ES growth media without LIF for 48 h to form EBs in suspension[49]. The EBs were collected and allowed to sediment in falcon tubes where they were washed 2 times with PBS and then resuspended in serum replacement medium (2% serum replacement/DMEM supplemented with 1X Pen/Strep and L-Glutamine and 0.45mM Monothioglycerol) containing FGF 10ng/ml (Catalogue) and 50ng/ml A. The EBs were then transferred to new bacterial dishes and maintained for an additional 48h prior to imagining under an inverted fluorescent microscope using the Infinity3 camera (Lumenera, Canada). EB's were then centrifuged, washed in PBS and RNA or for protein extraction for further analysis.

RNA sequencing: ESCs were separated from feeders by pre-plating as above then cultured in 2i medium consisting of N2B27 supplemented with Glutamine and Pen/Strep, 50uM β-mercaptoethanol, 3μM CHIRON (Cayman Chemical, 13122), 1μM PD03 (Sigma Aldrich, PZ0162) and LIF (homemade). Cells were trypsinised and plated into Cellbind dishes (Corning, 734-4057) coated with 40ug/dish fibronectin (Millipore, FC010) at a concentration of 3X10^6 cells per dish in N2B27 medium without 2i. 24 h later, cells were switched to fresh N2B27 medium containing 10μM SB43152 for 4 h

to inhibit endogenous TGFβ signalling. Cells were washed 2 times in PBS and then treated with 10ng/mL Activin A for 3 or 6 h or SB431542 for 3 hours prior to harvesting for RNA as described for qPCR (see mouse and embryo methods). The integrity of the RNA was checked using Agilent 2100 Bioanalyser and a total of 1 ug RNA with a RIN>8 was used for sequencing. RNA sequencing was performed by GATC Biotech (Constance, Germany). In ESCs treated in parallel were processed for western blot analysis.

CRISPR-Cas9: CRISPR guide RNAs (sgRNA) were designed using the Feng Zhang lab Target Finder design tool (http://crispr.mit.edu/). We designed a total of 4 guideRNA primer pairs for each gene to create a deletion in the first coding exon. Individual guide sequences are shown in Extended data Table 2. Each guide oligonucleotide was purchased with its complementary oligonucleotide (Sigma Aldrich) and annealed using the T4 Polynucleotide Kinase Kit (New England Biolab, M0201). Annealed guides were then cloned into the pSpCas9(BB)-2A-Puro (PX459) V2.0 (Addgene, plasmid 62988, PMID: 24157548). *Ark* -/- MEFs were transfected with 4 guide pairs in order to create the desired deletion using FUGENE (Promega, E2311) according to manufacturer's instructions. The following day, cells were trypsinised and seeded into 10cm dishes at different cell densities. 36 hours post transfection, cells were switched to culture medium containing 3µg/ml of puromycin for 48 hrs to select individual clones. Clones were screened for deletions using DNA-PCR analysis with primer pairs flanking the region targeted by the guide-RNAs. The deleted clones were analysed by western blot to confirm loss of the proteins generated by CRISPR gene-knockout.

To create the SnoN deletion in ESCs, the Ark-/- ESC-line 39 (A-/- 39) was used. ESCs were weaned from feeders and cultured in 2i medium plus LIF on gelatinised Cellbind dishes (as described for RNA sequencing) for transfection and puromycin selection. The same guide-RNA plasmids were used as for MEFs, but the transfection was performed by nucleofection according to manufacturer's instructions for the Nucleofector™ 2b Device (Lonza) and the Mouse ES cell Nucleofector kit (Lonza, Cat No. VPH-1001). 36 hours after transfection the cells were selected by 2µg/ml puromycin for 48 hours. Colonies were transferred onto 96 well plates with feeders on DMEM-LIF medium as before the transfection for expansion.

FIGURE LEGENDS

FIGURE 1: **Arkadia functions via SNON in embryonic cells**. (a) Transcriptional responses measured by luciferase assay in MEFs treated with either SB (SB431542) inhibitor or increasing concentration (ng/ml) of TGFβ ligand. Note the recovery of the luciferase activity with ligand treatment in [*SnoN/Ark*] double-null MEFs compared to *Ark-/-.* (b) *Hex-Gfp* transgenic ESC differentiated towards ADE via Embryoid bodies (EB). Fluorescence and bright field images on the left and right respectively. (c) QPCR expression analysis of definitive endoderm and ME markers performed on the above-differentiated EBs. Note the recovery of ADE marker expression in double null EBs. (d) Western blot analysis with antibodies as indicated on extracts from E8.5 embryos with genotype as indicated. Note the upregulation of SKI in *SnoN*-/- embryos.

FIGURE 2: **Arkadia functions via SNON in the embryo.** Images of embryos with genotypes as indicated, stained with various markers by WISH. (a) *Cerberus* expression in E7.5 embryos. The arrow points to the AVE and the arrowhead to the ADE. Anterior side of the embryos is at the left, posterior to the right. The scale bar is 100μm. (b) *Six3* expression in E8.5 embryos. The scale bar is 200μm. (c) *Foxa2* expression in E8.5 embryos. Lateral view is shown in the top panel, and ventral view in the bottom. Arrows point to the ME. The scale bar is 200μm. (d) *Shh* expression in E9 embryos. Lateral view of the embryos is shown. The arrow points to the posterior-endoderm and the arrowhead to the ME. The scale bar is 200μm. Note the rescue of tissue-development in [*SnoN/Ark*]-/- embryos compared to *Ark*-/- for all tissues examined with the above markers. The expression of Six3 may be marginally less in [*SnoN/Ark*]-/- compared to *Wt* embryos but WISH is semiquantitative suggesting that it is not significant.

FIGURE 3: **Arkadia derepresses SNON repressed genes**. (a) Western blot with antibodies against SKI, SNON, SMAD2 (pS2), total SMAD2/3 (S2/3) and β-ACTIN, on extracts from ESCs with genotypes as indicated, and treated over time as indicated. (b) Expression graphs (trend lines) of representative Arkadia dependent and independent SMAD2/3-induced targets. The data derive from the RNA-sequencing data. (c) Graph of Activin (AA)-induction differences (FC) at T3 and T6 of all Arkadia-dependent (Ark-Dep.) targets, which were identified on the basis of exhibiting ≥ 1.5-

fold (dotted line) induction difference between *Wt* and Ark-/- ESCs at T3. Note that the genes with asterisks become Arkadia independent at T6. (d) QPCR expression analysis of representative Arkadia dependent targets in *Wt*, *Ark*-/- and [*SnoN/Ark*]-/- ESCs showing recovery of signalling induction in the double null cells.

FIGURE 4: **SMAD2/3 levels drive equal SNON degradation**. (a) Western blot analysis with antibodies SMAD2 (pS2), total SMAD2/3 (S2/3), SNON and β-Actin on extracts from ESCs treated with TGFβ ligand over time after pretreatment for 4h with inhibitor SB, which is represented with zero "0" time point. Note that SKI and SNON exhibit slight reduction in the *Ark-/-* ESCs with signalling over time suggesting that Arkadia is the major E3-biquitin ligases that degrades them. (b) Images of PLA experiments with pairs of antibodies S2/3 and SMAD4 (S4) in (b); and S2/3 and SNON in (c) on *Wt* and *Ark*-/- MEFs treated with SB inhibitor or TGFβ as indicated.

FIGURE 5: **SMAD2/3 levels drive derepression**. (a) Western blot analysis with antibodies as indicated on extracts from *Wt*-ESCs treated with Activin ligand titrated with different levels of SB inhibitor, as indicated. Graphs showing the quantification of SMAD2 (pS2) and SNON proteins, and the pS2/SNON ratio of the proteins on the above blot in (b) and (c) respectively. (d) QPCRs expression analysis for known SMAD2/3 target genes, as indicated, on *Wt* ESCs treated with Activin titrated with SB inhibitor, as indicated. (e) Model showing on the left panel that SNON-SMAD4 complexes repress a subset of SMAD2/3 induced genes in the absence of signalling; middle panel shows conditions of low signalling where Arkadia degrades SNON-SMAD2/3 complexes but SMAD2/3 is not enough to eliminate all SNON and therefore SMAD4-SNON repression persists. The right panel shows the high signalling condition, where SMAD2/3 levels are higher than SNON enabling Arkadia to eliminate SNON leading to derepression.

EXTENDED DATA FIGURE 1: (a) *CAGA$_{12}$-luciferase* reporter assay in MEFs treated with SB inhibitor or increasing concentrations of TGFβ ligand, showing that *Ark*-/- MEFS do not respond to the ligand (b) *CAGA$_{12}$-luciferase* reporter assay in three different *SnoN*-CRISPR clones generated in *Ark*-/- MEFs, [*SnoN/Ark*]-/-, treated with TGFβ ligand showing rescue of the activity compared to *Ark*-/- null MEFs. (c) Western blot showing loss of SNON protein in the above three [*SnoN/Ark*]-/- CRISPR clones compared to *Wt* and *SnoN*-/- MEFs. β-ACTIN was used as loading control. (d) *CAGA$_{12}$-*

luciferase reporter assay showing rescue of the activity with TGFβ-ligand treatment in *Ark*-/- MEFs transfected with plasmid expressing Arkadia (*Wt-Ark*) but not with empty vector or with enzymatically mutant Arkadia (*RingMut)*. (e) *CAGA$_{12}$-luciferase* reporter assay showing comparable response in *Wt* and *SnoN*-/- MEFs upon TFβ-ligand stimulation.

EXTENDED DATA FIGURE 2: (a) Sequencing of three *Smad7*-CRISPR clones generated in *Ark*-/- MEFs confirmed various deletions in the sequence between the two gRNA sequences (in yellow and read fond). (b) *CAGA$_{12}$-luciferase* reporter assay in above three [*Smad7/Ark*]-/- MEF-clones showing no rescue because there is no response after treatment with increasing concentration of TGFβ ligand. (c) Western blot showing loss of SKI protein in three *Ski*-CRISPR clones generated in *Ark*-/- MEFs. β-ACTIN was used as loading control. (d) *CAGA$_{12}$-luciferase* reporter assay in the above three different [*Ski/Ark*]-/- MEF-clones showing no rescue because there is no response after treatment with increasing concentration of TGFβ ligand.

EXTENDED DATA FIGURE 3: (a) Western blot showing loss of SNON protein in 10 *SnoN*-CRISPR clones generated in one *Ark*-/- ESC-line. (b) Western blot with GFP antibody on EBS carrying *Hex-Gfp* differentiated towards ADE-ME showing rescue of differentiation in [*SnoN/Ark*]-/- EBs. (c) Images of GFP fluorescence in EBs derived from ESC-lines carrying *Hex-Gfp* differentiated towards ADE-ME showing that three *SnoN*-/- ESC-lines exhibit ability to differentiate comparable to *Wt*. (d) qPCR on the above EBs (c) with definitive endoderm (*Cscr4*) and ME (*Foxa2*) markers confirming the differentiation.

EXTENDED DATA FIGURE 4: (a) Agarose gel and schematic representation show the *in situ* probe generated from the first coding exon of *SnoN* gene containing all the conserved domains interacting with SMAD2/3, SMAD4 and histone deacetylases. Green arrows indicate the primers used; the blue box indicates the replacement of the *SnoN*-exon with the *β-galactosidase* gene (*LacZ*) containing nuclear localisation signal (NLS) present in the *Ski^{tm2Spw}* allele. (b) Images of WISH stained E8.5 mouse embryos with the above probe showing staining in *Wt* but not in the homozygous for *Ski^{tm2Spw}* allele. (c) Images of a 2-somite E8.5 embryos (right panel) and late head-fold E7.5 (left panel) heterozygous for *SnoN-$^{NSL\text{-}lacZ}$* allele stained with X-gal for <30'. Limiting the X-gal staining to the period that it is linear allows quantification of expression levels differences. The NLS-lacZ gene insertion is promoterless and it is therefore expressed via the endogenous *SnoN* gene. Arrows and arrowhead indicate high levels of *SnoN*-expression in the node and ADE. (d) Images of WISH with ADE marker, *Cerberus* probe on eight *Wt* and eight *SnoN*-/- embryos stages between E7-E7.5. Arrowheads

and Arrows indicate ADE and AVE respectively. The scale bar is 100µm. Embryos are positioned with anterior on the left and posterior to the right. (e) X-gal stained E.8.5 embryos showing rescue of head and midline in [*SnoN/Ark*]-/-. (f) X-gal stained E9 embryos showing no rescue in [*Smad7/Ark*]-/-. Like the *SnoN*-null allele, the *Ark*-null allele contains a promoterless *β-galactosidase* gene expressed via the endogenous promoter.

EXTENDED DATA FIGURE 5: (a) QPCRs on embryos (each dot represents different embryo) with a genotype as indicated. (b) QPCRs analysis of the responses under signalling induction in ESCs lines treated with SB inhibitor (4hr) or Activin (3hr). The ESC-line genotype is indicated along with the target gene used. (c) Heat-map of all SMAD2/3 induced genes identified by the RNA-sequencing experiment and selected on the basis that they exhibit more than 2-fold induction difference between T3 (Activin for 3h) and T0 (SB) in both Wt ESC-lines. They are ranked on the heat-map by the induction difference between *Wt* and *Ark*-/- at T3.

EXTENDED DATA FIGURE 6: (a and b) Heat-map of Arkadia dependent targets exhibiting ≥1.6 or ≥1.9 induction difference between *Wt* and *Ark*-/- ESCs as this is judged by comparing the fold change between T0 and T3 expression levels. All genes shown in this study are SMAD2/3 targets because they exhibit ≥2-fold induction with Activin at T3 in both *Wt* ESC lines.

EXTENDED DATA FIGURE 7: (a) Graphs of representative Arkadia dependent and independent SMAD2/3 targets because they are induced ≥2-fold by Activin at T3. (b) Western blot analysis of E8.5 embryo extracts with SMAD2 (pS2) antibody and PCNA as loading control. The genotype of the embryos is as indicated showing accumulation of SMAD2 in the absence of Arkadia. (c) Western blot analysis with antibodies pS2, total SMAD2/3 (S2/3), SNON and β-Actin on extracts from *Wt*-ESCs treated with TGFβ ligand titrated with different levels of SB inhibitor, as indicated.

EXTENDED DATA TABLE 1: RNA-sequencing results showing the expression profile of genes (in FPKM) over time under treatment with SB inhibitor (T0) or Activin for 3hrs (T3) or 6hrs (T6) in two different *Wt* ESC-lines: WT-18 and WT-26 and two different *Ark*-/- ESC-lines: A-/- 25 and A-/- 39. The genes on this list are considered as SMAD2/3 targets because they are all induced ≥2-fold by Activin in both *WT* ESC lines at T3.

EXTENDED DATA TABLE 2: Primers used in methods

REFERENCES

1 Massague, J., Seoane, J. & Wotton, D. Smad transcription factors. *Genes Dev* **19**, 2783-2810, doi:10.1101/gad.1350705 (2005).

2 Macias, M. J., Martin-Malpartida, P. & Massague, J. Structural determinants of Smad function in TGF-beta signaling. *Trends Biochem Sci* **40**, 296-308, doi:10.1016/j.tibs.2015.03.012 (2015).

3 Hill, C. S. Transcriptional Control by the SMADs. *Cold Spring Harb Perspect Biol* **8**, doi:10.1101/cshperspect.a022079 (2016).

4 Budi, E. H., Duan, D. & Derynck, R. Transforming Growth Factor-beta Receptors and Smads: Regulatory Complexity and Functional Versatility. *Trends Cell Biol* **27**, 658-672, doi:10.1016/j.tcb.2017.04.005 (2017).

5 Deheuninck, J. & Luo, K. Ski and SnoN, potent negative regulators of TGF-beta signaling. *Cell Res* **19**, 47-57, doi:10.1038/cr.2008.324 (2009).

6 Morikawa, M., Koinuma, D., Miyazono, K. & Heldin, C. H. Genome-wide mechanisms of Smad binding. *Oncogene* **32**, 1609-1615, doi:10.1038/onc.2012.191 (2013).

7 Robertson, E. J. Dose-dependent Nodal/Smad signals pattern the early mouse embryo. *Semin Cell Dev Biol* **32**, 73-79, doi:10.1016/j.semcdb.2014.03.028 (2014).

8 Zinski, J., Tajer, B. & Mullins, M. C. TGF-beta Family Signaling in Early Vertebrate Development. *Cold Spring Harb Perspect Biol* **10**, doi:10.1101/cshperspect.a033274 (2018).

9 Sagner, A. & Briscoe, J. Morphogen interpretation: concentration, time, competence, and signaling dynamics. *Wiley Interdiscip Rev Dev Biol* **6**, doi:10.1002/wdev.271 (2017).

10 van Boxtel, A. L., Economou, A. D., Heliot, C. & Hill, C. S. Long-Range Signaling Activation and Local Inhibition Separate the Mesoderm and Endoderm Lineages. *Dev Cell* **44**, 179-191 e175, doi:10.1016/j.devcel.2017.11.021 (2018).

11 Rogers, K. W. *et al.* Nodal patterning without Lefty inhibitory feedback is functional but fragile. *Elife* **6**, doi:10.7554/eLife.28785 (2017).

12 Papatsenko, D. & Levine, M. Quantitative analysis of binding motifs mediating diverse spatial readouts of the Dorsal gradient in the Drosophila embryo. *Proc Natl Acad Sci U S A* **102**, 4966-4971, doi:10.1073/pnas.0409414102 (2005).

13 Jazwinska, A., Kirov, N., Wieschaus, E., Roth, S. & Rushlow, C. The Drosophila gene brinker reveals a novel mechanism of Dpp target gene regulation. *Cell* **96**, 563-573 (1999).

14 Campbell, G. & Tomlinson, A. Transducing the Dpp morphogen gradient in the wing of Drosophila: regulation of Dpp targets by brinker. *Cell* **96**, 553-562 (1999).

15 Minami, M., Kinoshita, N., Kamoshida, Y., Tanimoto, H. & Tabata, T. brinker is a target of Dpp in Drosophila that negatively regulates Dpp-dependent genes. *Nature* **398**, 242-246, doi:10.1038/18451 (1999).

16 Arkell, R. M. & Tam, P. P. Initiating head development in mouse embryos: integrating signalling and transcriptional activity. *Open Biol* **2**, 120030, doi:10.1098/rsob.120030 (2012).

17 Dunn, N. R., Vincent, S. D., Oxburgh, L., Robertson, E. J. & Bikoff, E. K. Combinatorial activities of Smad2 and Smad3 regulate mesoderm formation and patterning in the mouse embryo. *Development* **131**, 1717-1728, doi:10.1242/dev.01072 (2004).

18 Kinder, S. J. *et al.* The organizer of the mouse gastrula is composed of a dynamic population of progenitor cells for the axial mesoderm. *Development* **128**, 3623-3634 (2001).

19 Episkopou, V. *et al.* Induction of the mammalian node requires Arkadia function in the extraembryonic lineages. *Nature* **410**, 825-830, doi:10.1038/35071095 (2001).

20 Mavrakis, K. J. *et al.* Arkadia enhances Nodal/TGF-beta signaling by coupling phospho-Smad2/3 activity and turnover. *PLoS Biol* **5**, e67, doi:10.1371/journal.pbio.0050067 (2007).

21 Niederlander, C., Walsh, J. J., Episkopou, V. & Jones, C. M. Arkadia enhances nodal-related signalling to induce mesendoderm. *Nature* **410**, 830-834, doi:10.1038/35071103 (2001).

22 Koinuma, D. *et al.* Arkadia amplifies TGF-beta superfamily signalling through degradation of Smad7. *EMBO J* **22**, 6458-6470, doi:10.1093/emboj/cdg632 (2003).

23 Levy, L. *et al.* Arkadia activates Smad3/Smad4-dependent transcription by triggering signal-induced SnoN degradation. *Mol Cell Biol* **27**, 6068-6083, doi:10.1128/MCB.00664-07 (2007).

24 Nagano, Y. *et al.* Arkadia induces degradation of SnoN and c-Ski to enhance transforming growth factor-beta signaling. *J Biol Chem* **282**, 20492-20501, doi:10.1074/jbc.M701294200 (2007).

25 Affolter, M. & Basler, K. The Decapentaplegic morphogen gradient: from pattern formation to growth regulation. *Nat Rev Genet* **8**, 663-674, doi:10.1038/nrg2166 (2007).

26 Le Scolan, E. *et al.* Transforming growth factor-beta suppresses the ability of Ski to inhibit tumor metastasis by inducing its degradation. *Cancer Res* **68**, 3277-3285, doi:10.1158/0008-5472.CAN-07-6793 (2008).

27 Sharma, V. *et al.* Enhancement of TGF-beta signaling responses by the E3 ubiquitin ligase Arkadia provides tumor suppression in colorectal cancer. *Cancer Res* **71**, 6438-6449, doi:10.1158/0008-5472.CAN-11-1645 (2011).

28 Briones-Orta, M. A. *et al.* Arkadia regulates tumor metastasis by modulation of the TGF-beta pathway. *Cancer Res* **73**, 1800-1810, doi:10.1158/0008-5472.CAN-12-1916 (2013).

29 Morrison, G. M. *et al.* Anterior definitive endoderm from ESCs reveals a role for FGF signaling. *Cell Stem Cell* **3**, 402-415, doi:10.1016/j.stem.2008.07.021 (2008).

30 Ang, S. L. *et al.* The formation and maintenance of the definitive endoderm lineage in the mouse: involvement of HNF3/forkhead proteins. *Development* **119**, 1301-1315 (1993).

31 Pearson-White, S. & McDuffie, M. Defective T-cell activation is associated with augmented transforming growth factor Beta sensitivity in mice with mutations in the Sno gene. *Mol Cell Biol* **23**, 5446-5459 (2003).

32 Belo, J. A. *et al.* Cerberus-like is a secreted factor with neutralizing activity expressed in the anterior primitive endoderm of the mouse gastrula. *Mech Dev* **68**, 45-57 (1997).

33 Oliver, G. *et al.* Six3, a murine homologue of the sine oculis gene, demarcates the most anterior border of the developing neural plate and is expressed during eye development. *Development* **121**, 4045-4055 (1995).

34 Echelard, Y. *et al.* Sonic hedgehog, a member of a family of putative signaling molecules, is implicated in the regulation of CNS polarity. *Cell* **75**, 1417-1430 (1993).

35 Tojo, M. *et al.* Smad7-deficient mice show growth retardation with reduced viability. *J Biochem* **151**, 621-631, doi:10.1093/jb/mvs022 (2012).

36 Guzman-Ayala, M. *et al.* Graded Smad2/3 activation is converted directly into levels of target gene expression in embryonic stem cells. *PLoS One* **4**, e4268, doi:10.1371/journal.pone.0004268 (2009).

37 Coda, D. M. *et al.* Distinct modes of SMAD2 chromatin binding and remodeling shape the transcriptional response to NODAL/Activin signaling. *Elife* **6**, doi:10.7554/eLife.22474 (2017).

38 Tecalco-Cruz, A. C. *et al.* Transforming growth factor-beta/SMAD Target gene SKIL is negatively regulated by the transcriptional cofactor complex SNON-SMAD4. *J Biol Chem* **287**, 26764-26776, doi:10.1074/jbc.M112.386599 (2012).

39 Zhang, S. *et al.* Reversing SKI-SMAD4-mediated suppression is essential for TH17 cell differentiation. *Nature* **551**, 105-109, doi:10.1038/nature24283 (2017).

40 Wrana, J. L. Signaling by the TGFbeta superfamily. *Cold Spring Harb Perspect Biol* **5**, a011197, doi:10.1101/cshperspect.a011197 (2013).

41 Zhu, Q. & Luo, K. SnoN in regulation of embryonic development and tissue morphogenesis. *FEBS Lett* **586**, 1971-1976, doi:10.1016/j.febslet.2012.03.005 (2012).

42 Gaarenstroom, T. & Hill, C. S. TGF-beta signaling to chromatin: how Smads regulate transcription during self-renewal and differentiation. *Semin Cell Dev Biol* **32**, 107-118, doi:10.1016/j.semcdb.2014.01.009 (2014).

43 Stroschein, S. L., Wang, W., Zhou, S., Zhou, Q. & Luo, K. Negative feedback regulation of TGF-beta signaling by the SnoN oncoprotein. *Science* **286**, 771-774 (1999).

44 Thymiakou, E. & Episkopou, V. Detection of signaling effector-complexes downstream of bmp4 using PLA, a proximity ligation assay. *J Vis Exp*, doi:10.3791/2631 (2011).

45 Meno, C. *et al.* lefty-1 is required for left-right determination as a regulator of lefty-2 and nodal. *Cell* **94**, 287-297 (1998).

46 Meno, C. *et al.* Mouse Lefty2 and zebrafish antivin are feedback inhibitors of nodal signaling during vertebrate gastrulation. *Mol Cell* **4**, 287-298 (1999).

47 Stuckey, D. W. *et al.* Coordination of cell proliferation and anterior-posterior axis establishment in the mouse embryo. *Development* **138**, 1521-1530, doi:10.1242/dev.063537 (2011).

48 Zieba, A. *et al.* Intercellular variation in signaling through the TGF-beta pathway and its relation to cell density and cell cycle phase. *Mol Cell Proteomics* **11**, M111 013482, doi:10.1074/mcp.M111.013482 (2012).

49 Brickman, J. M. & Serup, P. Properties of embryoid bodies. *Wiley Interdiscip Rev Dev Biol* **6**, doi:10.1002/wdev.259 (2017).

Figure 1

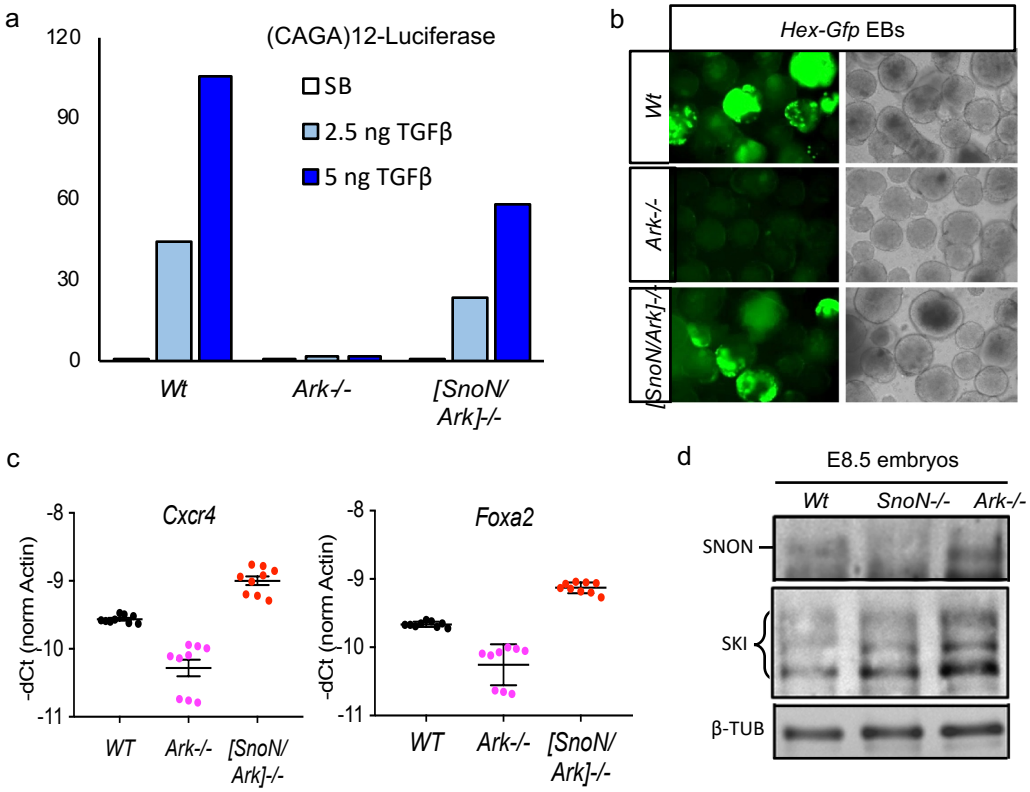
a
(CAGA)12-Luciferase
SB
2.5 ng TGFβ
5 ng TGFβ
120
90
60
30
0
Wt
Ark-/-
[SnoN/ Ark]-/-
b
Hex-Gfp EBs
Wt
Ark-/-
[SnoN/Ark]-/-
c
Cxcr4
Foxa2
-dCt (norm Actin)
-8
-9
-10
-11
WT
Ark-/-
[SnoN/ Ark]-/-
d
E8.5 embryos
Wt
SnoN-/-
Ark-/-
SNON
SKI
β-TUB

Figure 2

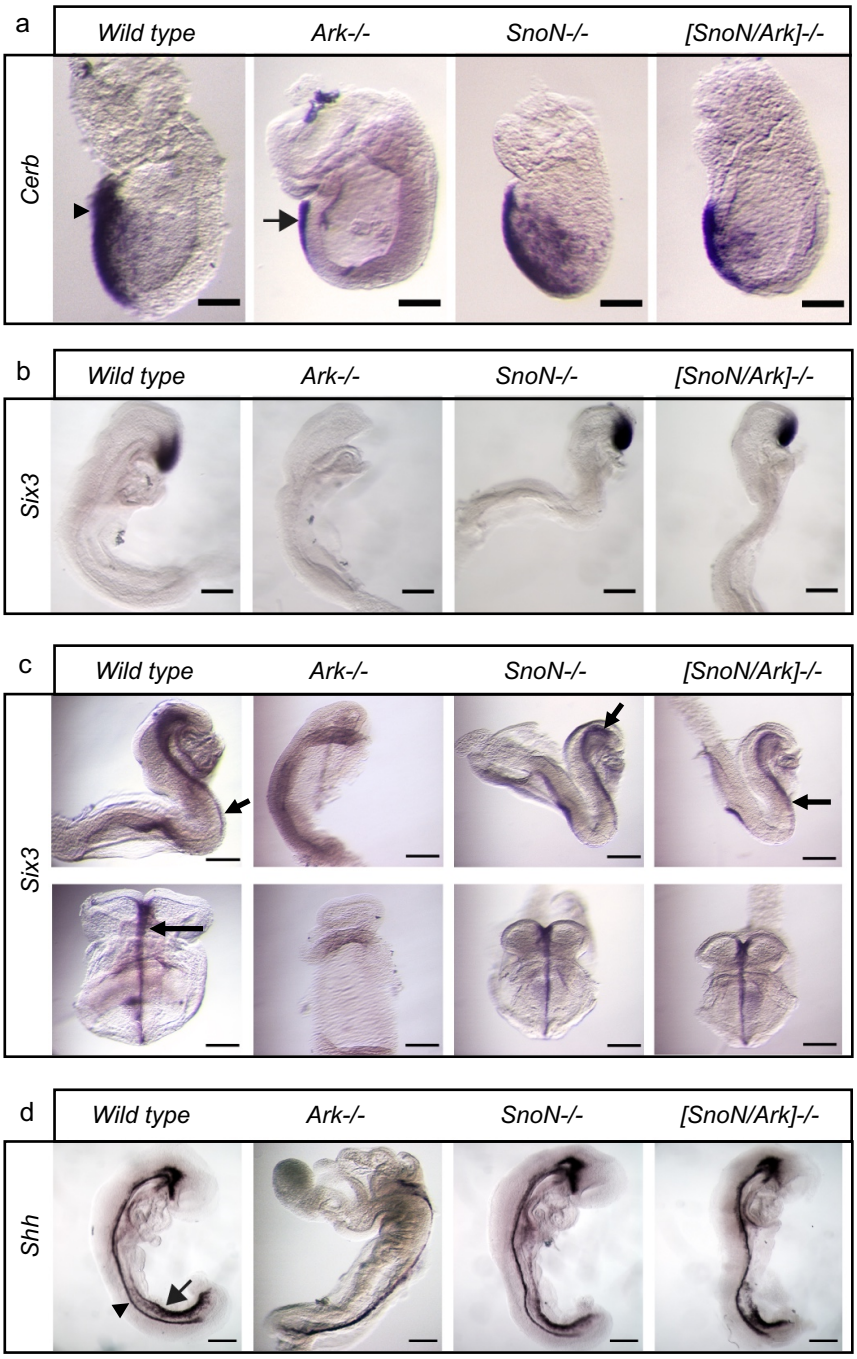
a
Wild type
Ark-/-
SnoN-/-
[SnoN/Ark]-/-
Cerb
b
Wild type
Ark-/-
SnoN-/-
[SnoN/Ark]-/-
Six3
c
Wild type
Ark-/-
SnoN-/-
[SnoN/Ark]-/-
Six3
d
Wild type
Ark-/-
SnoN-/-
[SnoN/Ark]-/-
Shh

Figure 3

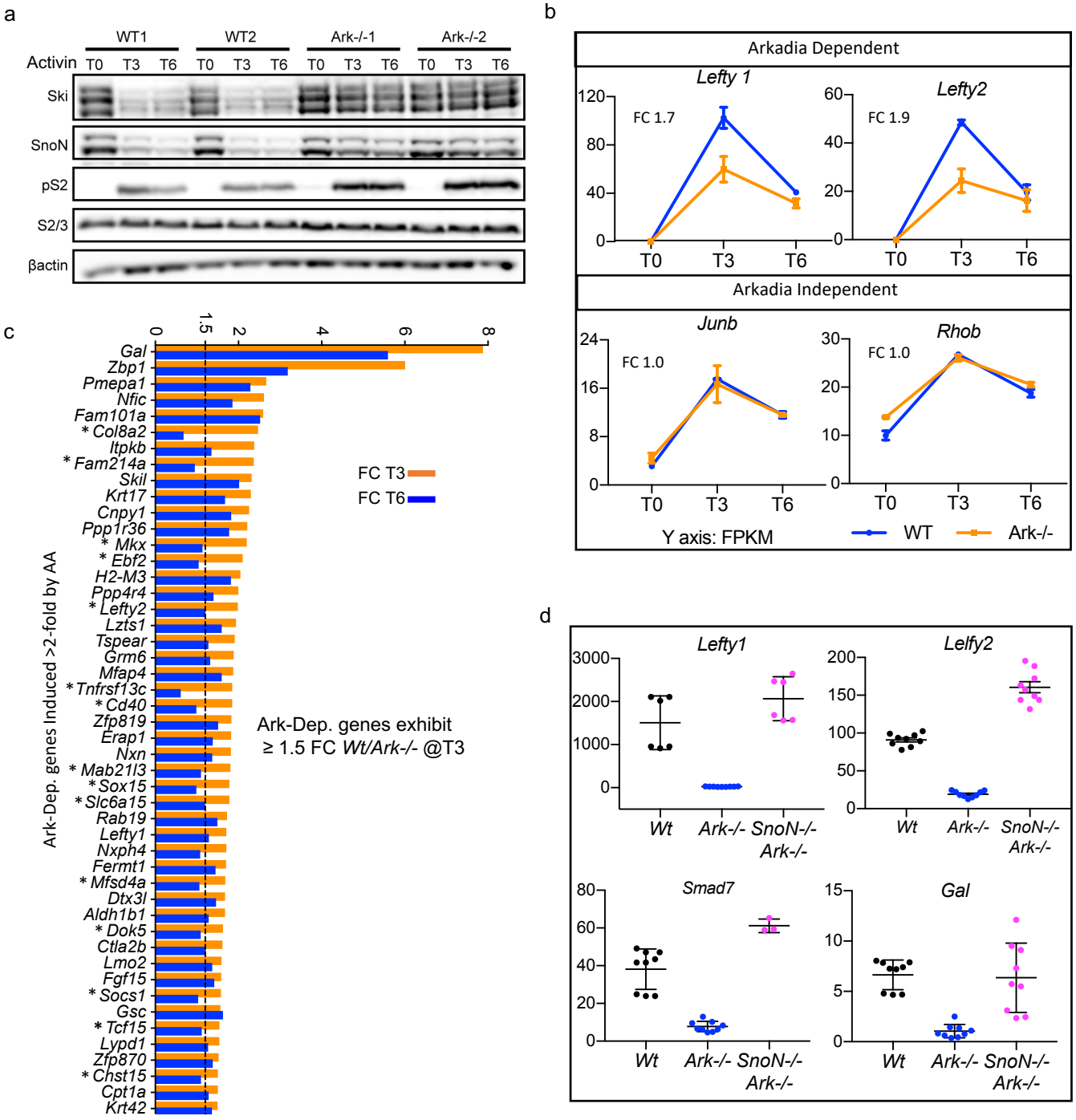
a
WT1
WT2
Ark-/-1
Ark-/-2
Activin
T0 T3 T6 T0 T3 T6 T0 T3 T6 T0 T3 T6
Ski
SnoN
pS2
S2/3
βactin
b
Arkadia Dependent
Lefty 1
FC 1.7
Lefty2
FC 1.9
Arkadia Independent
Junb
FC 1.0
Rhob
FC 1.0
T0 T3 T6
Y axis: FPKM
WT
Ark-/-
c
FC T3
FC T6
Ark-Dep. genes Induced >2-fold by AA
Gal
Zbp1
Pmepa1
Nfic
Fam101a
* Col8a2
Itpkb
* Fam214a
Skil
Krt17
Cnpy1
Ppp1r36
* Mkx
* Ebf2
H2-M3
Ppp4r4
* Lefty2
Lzts1
Tspear
Grm6
Mfap4
* Tnfrsf13c
* Cd40
Zfp819
Erap1
Nxn
* Mab21l3
* Sox15
* Slc6a15
Rab19
Lefty1
Nxph4
Fermt1
* Mfsd4a
Dtx3l
Aldh1b1
* Dok5
Ctla2b
Lmo2
Fgf15
* Socs1
Gsc
* Tcf15
Lypd1
Zfp870
* Chst15
Cpt1a
Krt42
Ark-Dep. genes exhibit
≥ 1.5 FC Wt/Ark-/- @T3
d
Lefty1
Lelfy2
Smad7
Gal
Wt
Ark-/-
SnoN-/-
Ark-/-

Figure 4

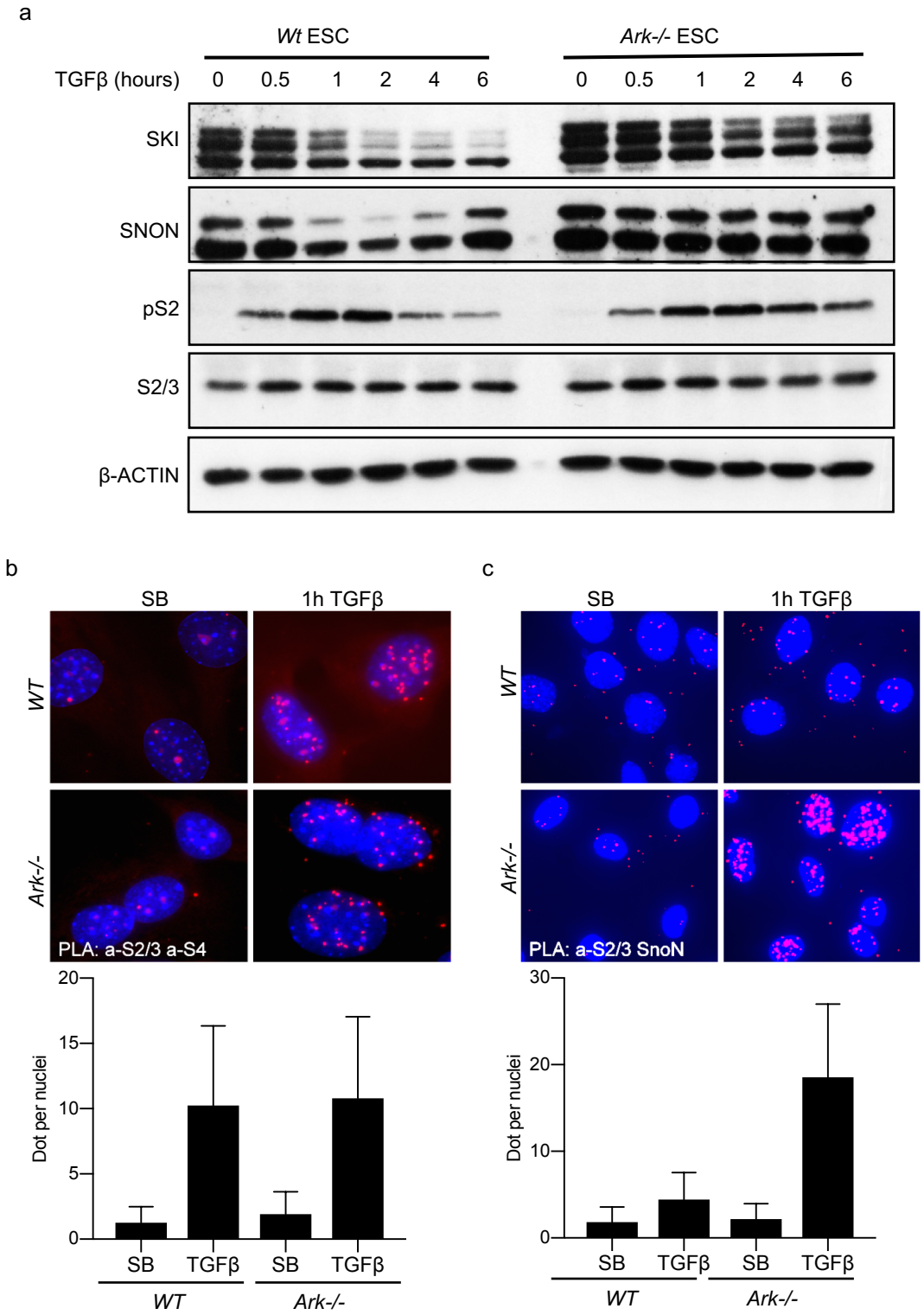
a
Wt ESC
Ark-/- ESC
TGFβ (hours)
0 0.5 1 2 4 6
0 0.5 1 2 4 6
SKI
SNON
pS2
S2/3
β-ACTIN
b
SB
1h TGFβ
WT
Ark-/-
PLA: a-S2/3 a-S4
Dot per nuclei
20
15
10
5
0
SB TGFβ SB TGFβ
WT
Ark-/-
c
SB
1h TGFβ
WT
Ark-/-
PLA: a-S2/3 SnoN
Dot per nuclei
30
20
10
0
SB TGFβ SB TGFβ
WT
Ark-/-

Figure 5

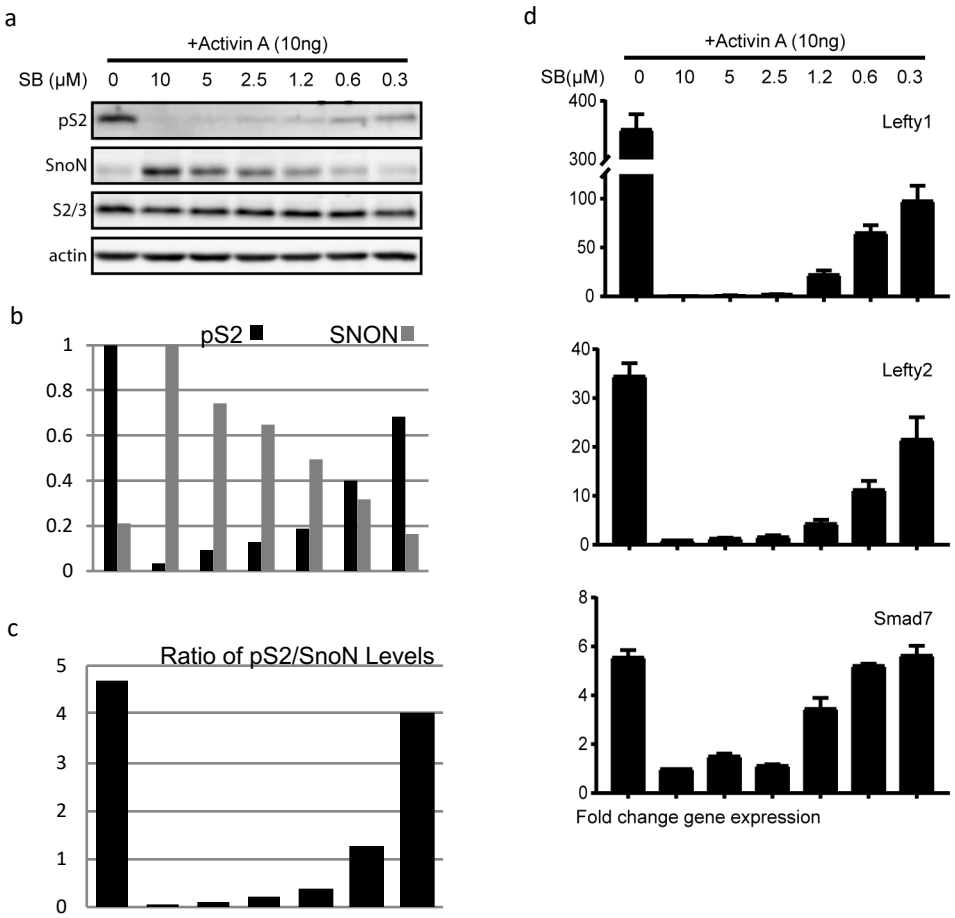
a
+Activin A (10ng)
SB (μM) 0 10 5 2.5 1.2 0.6 0.3
pS2
SnoN
S2/3
actin
b
pS2
SNON
1
0.8
0.6
0.4
0.2
0
c
Ratio of pS2/SnoN Levels
5
4
3
2
1
0
d
+Activin A (10ng)
SB(μM) 0 10 5 2.5 1.2 0.6 0.3
Lefty1
400
300
100
50
0
Lefty2
40
30
20
10
0
Smad7
8
6
4
2
0
Fold change gene expression

e

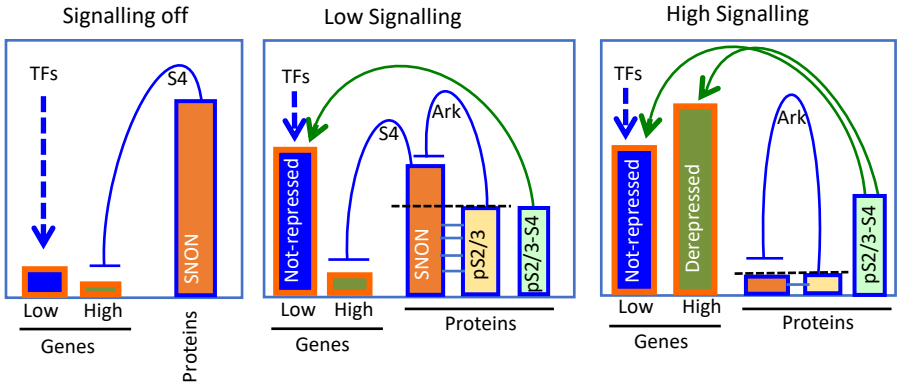
Signalling off
TFs
S4
SNON
Low
High
Genes
Proteins
Low Signalling
TFs
S4
Ark
Not-repressed
SNON
pS2/3
pS2/3-S4
Low
High
Genes
Proteins
High Signalling
TFs
Ark
Not-repressed
Derepressed
pS2/3-S4
Low
High
Genes
Proteins

Extended data Figure 1

a

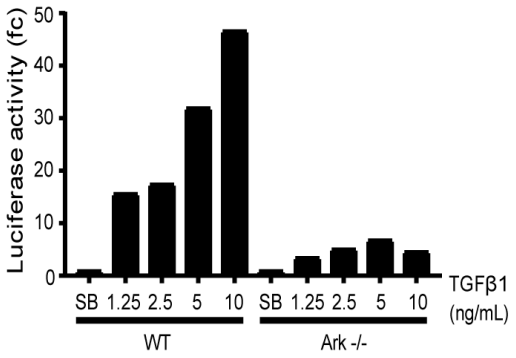

b

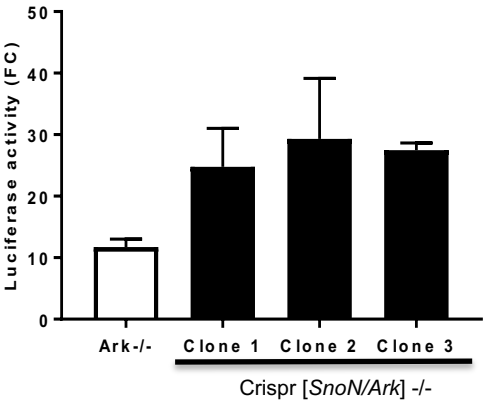

c

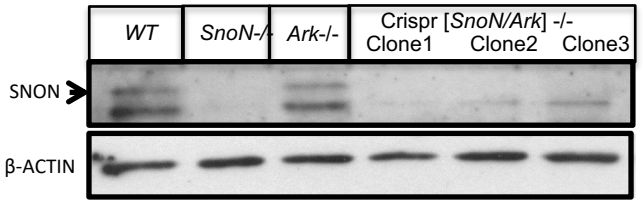

d

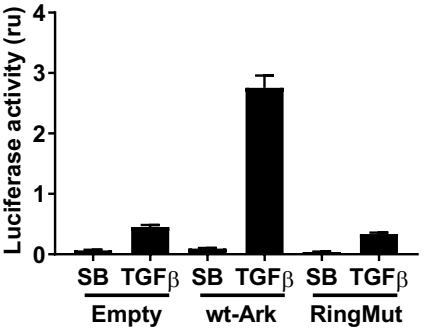

e

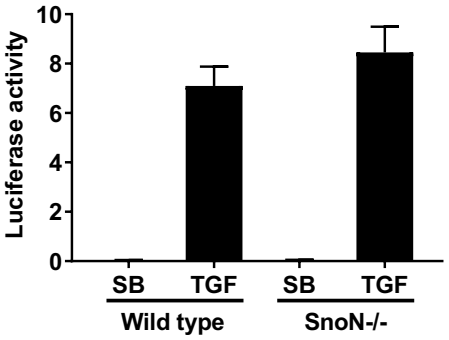

Extended data Figure 2

a

WT Smad7 sequence

```
CCCGGCAGGCGCCCCTGGGCCCCCGCGCGCGCCCCGGCCTCTGGGAGACTGGCGCATGCCACGGAGCGCCCCTCGGGCCGCC
GCCGCTTCTGCCCGGGCCCCTGCTGTTGCTGCTGTCGCCTGCGCCTGCTGCCCCAACTCGGCGCCCGACTTCTTCATGGTGT
GCGGAGGTCATGTTCGCTCCTTAGCCGGCAAACGACTTTTCTCCTCGCCTCCTCGCCCCGCATGTTCAGGACCAAACGATCT
GCGCTCGTCCGGCGTCTCTGGAGGAGCCGTGCGCCCGGCGGCGAGGACGAGGAGGAGGGCGTGGGGGGTGGCGGCGGAGGAG
GCGAGCTGCGGGGAGAAGGGGCGACGGACGGCCGGGCTTATGGGGCTGGTGGCGGCGGTGCGGGCAGGGCTGGCTGCTGCCT
GGGCAAGGCAGTCCGAGGTGCCAAAGGTCACCACCATCCCCATCCCCCAACCTCGGGTGCCGGGGCGGCCGGGGGCGCCGAG
GCGGATCTGAAGGCGCTCACGCACTCGGTGCTCAAGAAACTCAAGGAGCGGCAGCTGGAGCTGCTGCTTCAGGCCGTGGAGT
CCCGCGGCGGTACGCGCACCGCGTGCCTCCTGCTGCCCGGCCGCCTGGACTGCAGGCTGGGCCCGGGGGCGCCCGCCAGCGC
GCAGCCCGCGCAGCCGCCCTCGTCCTACTCGCTCCCCCTCCTGCTGTGCAAAGTGTTCAGGTGGCCGGATCTCAGGCATTCC
TCGGAAGTCAAGAGGCTGTGTTGCTGTGAATCTTACGGGAAGATCAACCCCGAGCTGGTGTGCTGCAACCCCCATCACCTTA
GTCGACTCTGTGAACTAGGTAAGAAGTTGTTCTGAGTCCACCTTTCGTTCCCTCTGGCGTGGAAATGCTCGAGGATGTGTGT
ATAACCTCCTGGAGGAGACAAGGAATCTAAGTCAGAGAAGGGACCAGGGGAAGCTTGGGGTTCCCTCTAAGATTTTTCTCTA
TTGCACCC
```

Smad7 Crispr KO sequence

```
TGAAGTACGACTTTTCTCCTCGCCTCCTCGCCCCGCATGTTCAGGACCAAACGATCTGCG
CTCGTCCGGCGTCTCTGGAGGAGCCGTGCGAGCTGGTGTGCTGCAACCCCCATCACCTTA
GTCGACTCTGTGAACTAGGTAAGAAGTTGTTCTGAGTCCACCTTTCGTTCCCTCTGGCGT
GGAAATGCTCGAGGATGTGTGTATAACCTCCTGGAGGAGACAAGGAATCTAAGTCAGAGA
AGGGACCAGGGGAACTTTGGGGTTCAATAACGCG
```

b

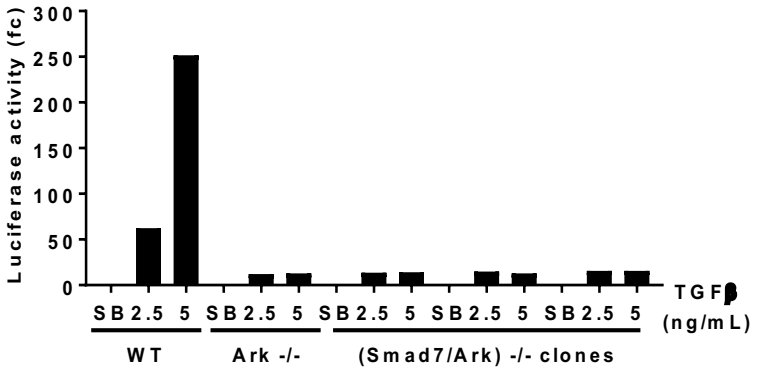

c

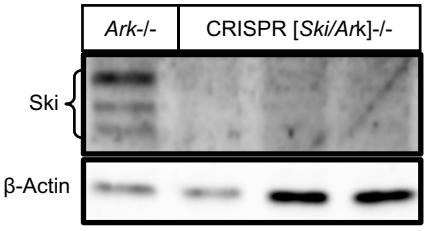

d

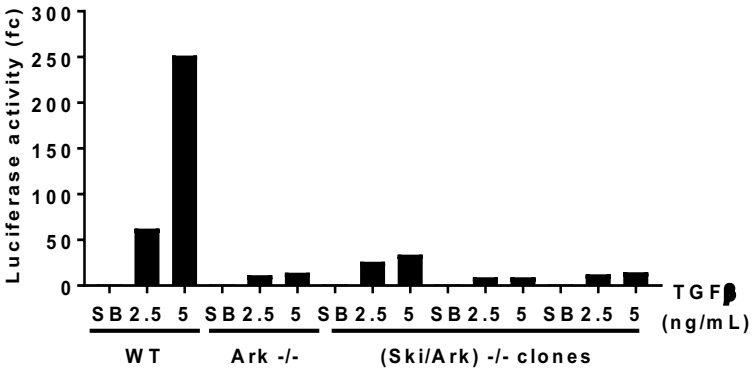

Extended data Figure 3

a

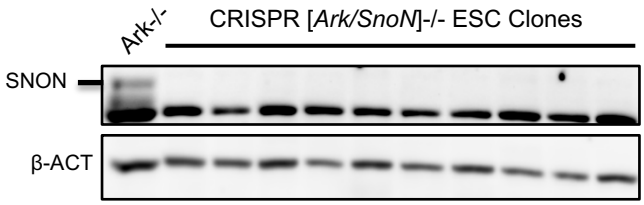

b

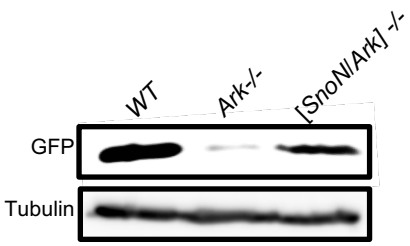

c

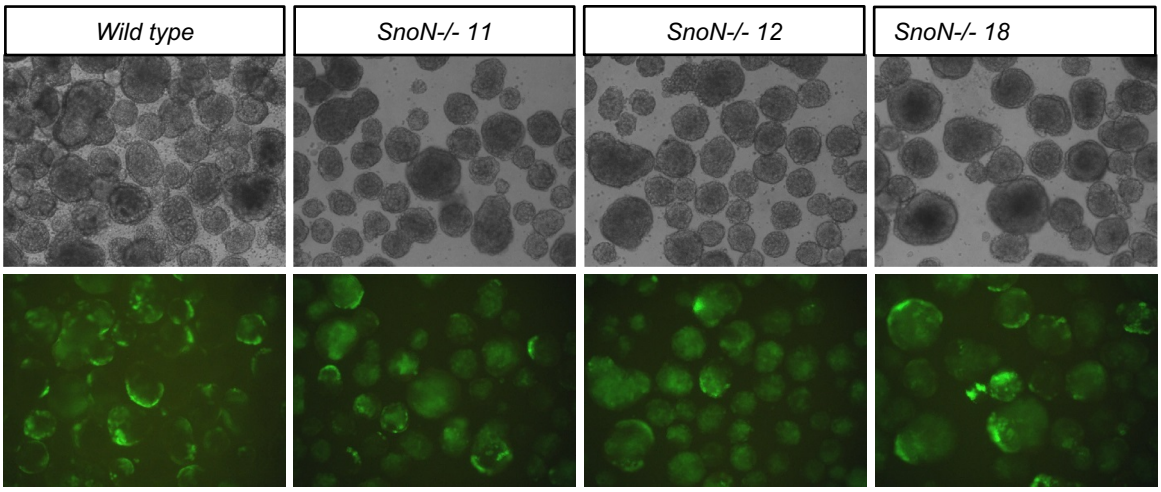

d

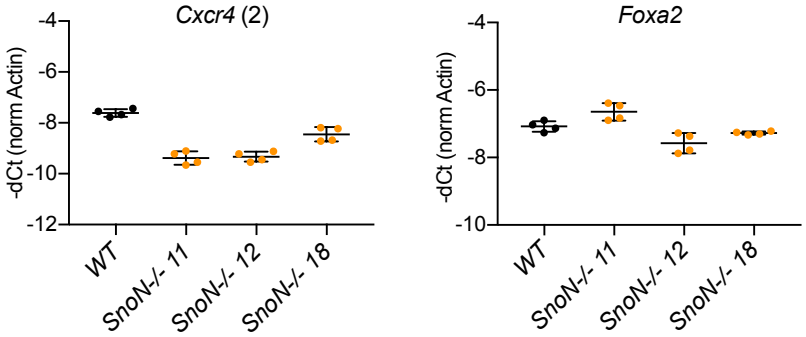

Extended data Figure 4

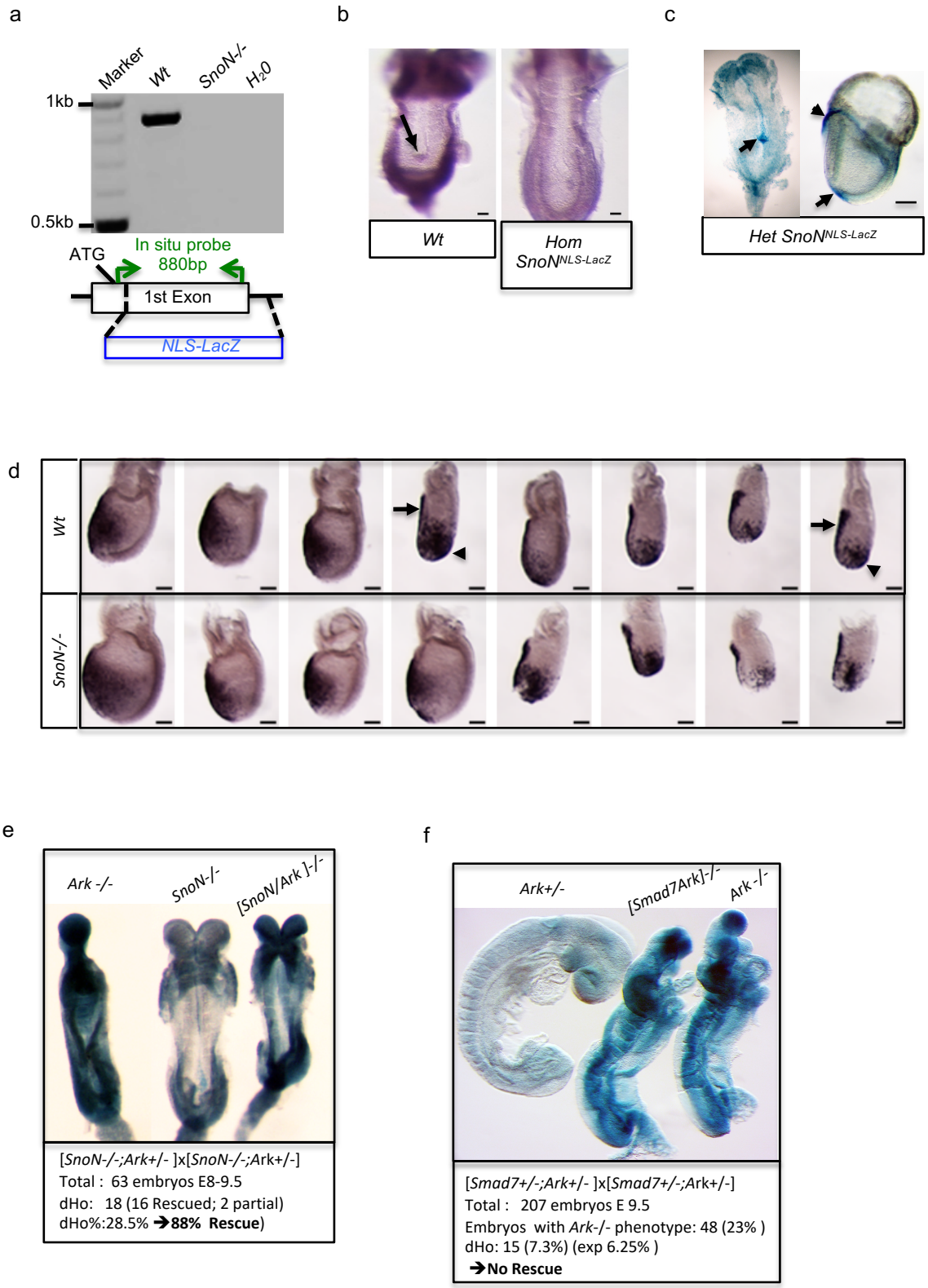

Extended data Figure 5

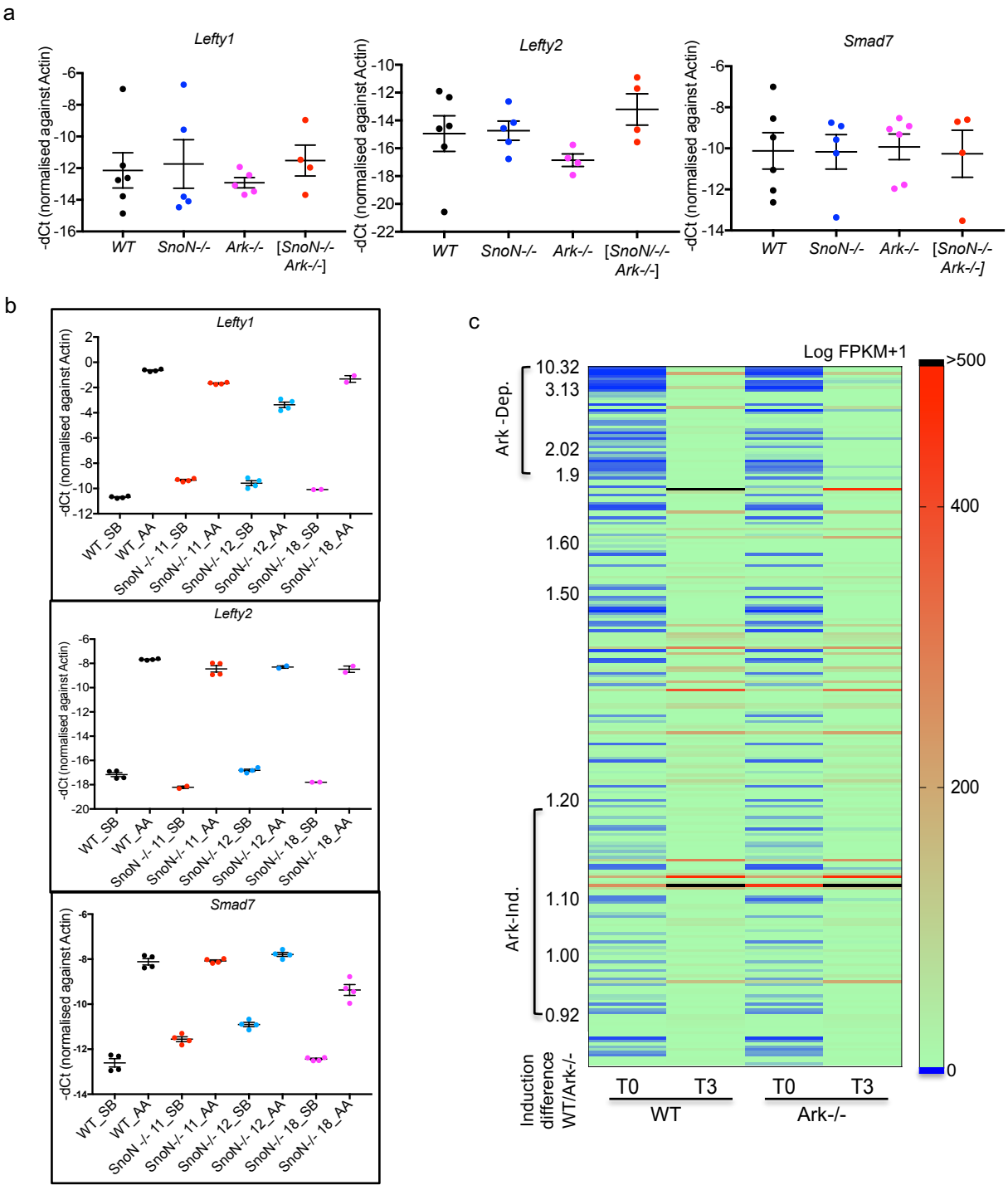

Extended data Figure 6

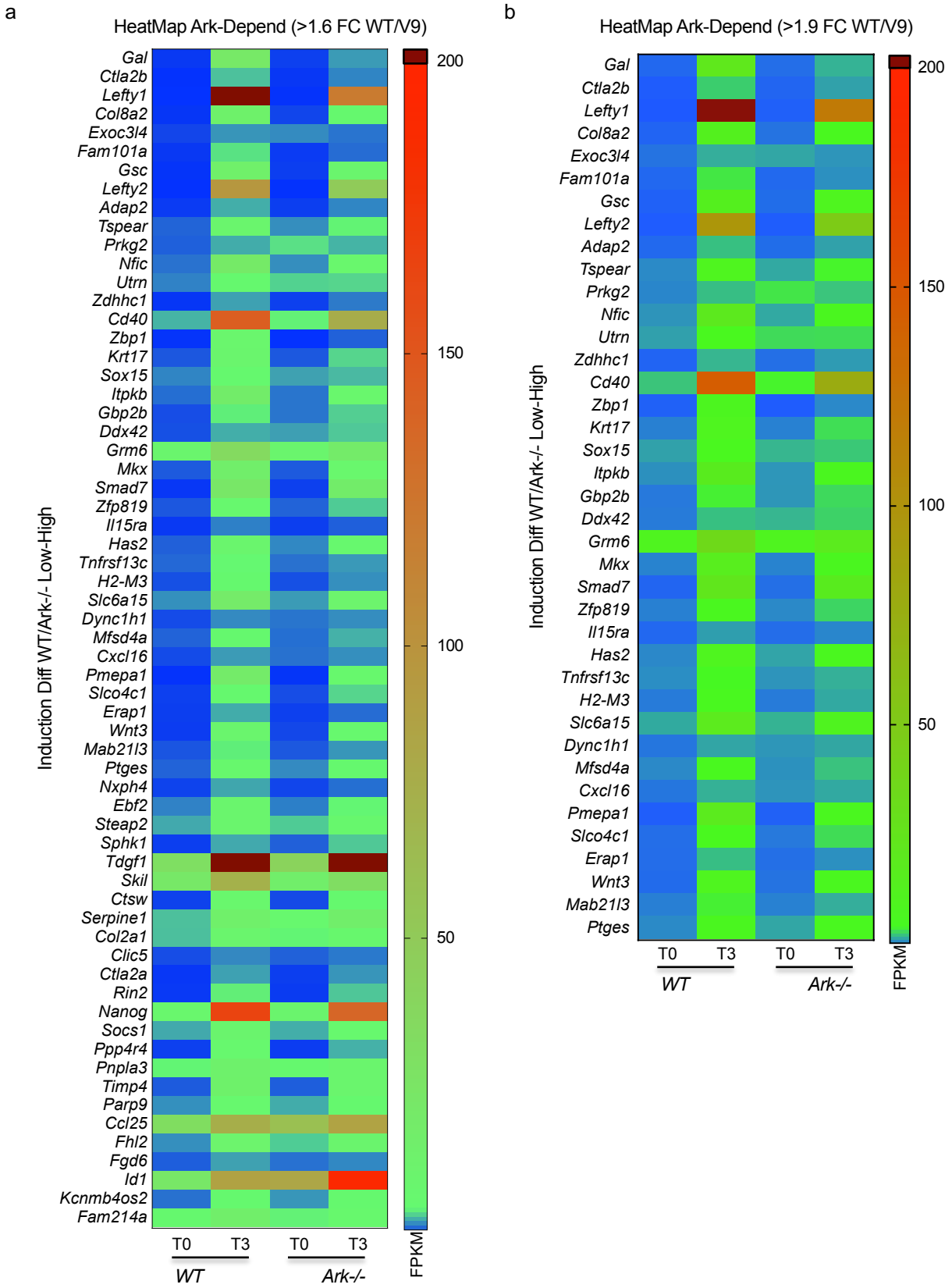

Extended data Figure 7

a

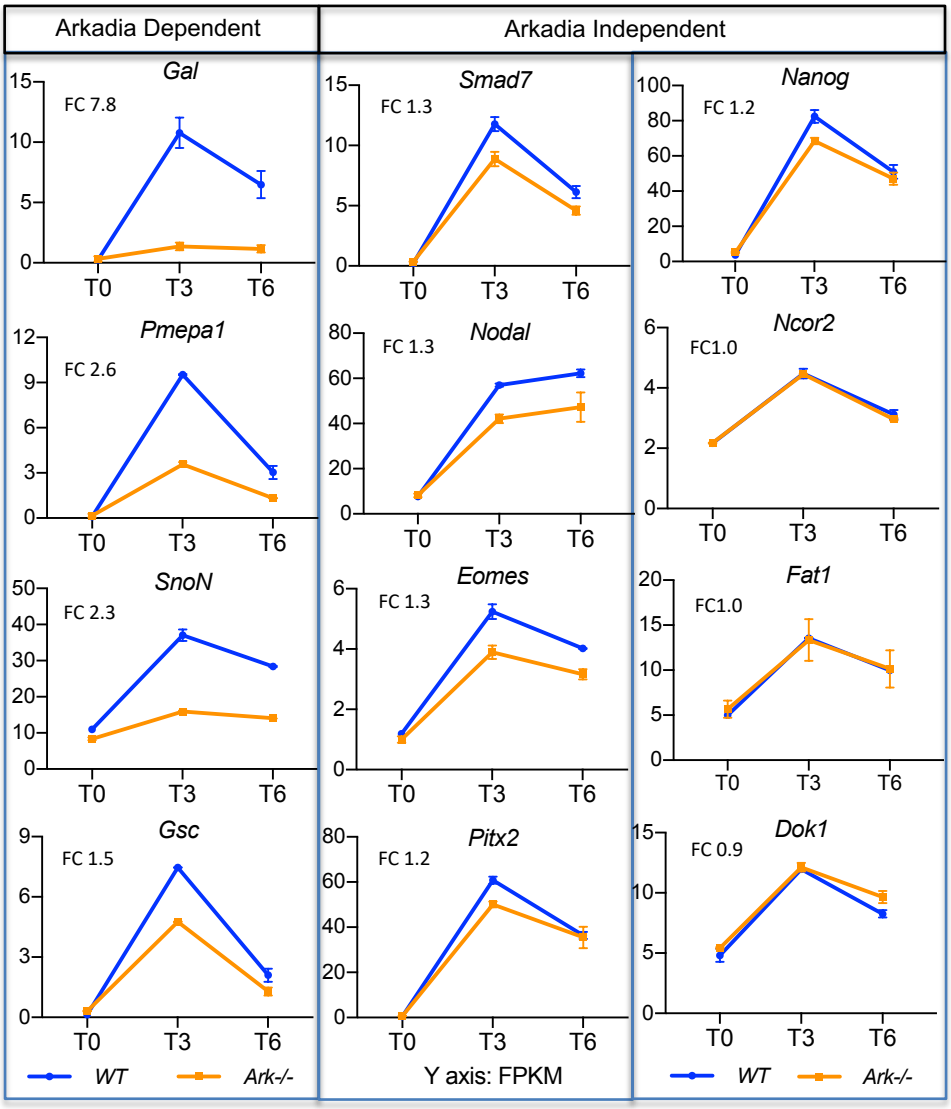

b

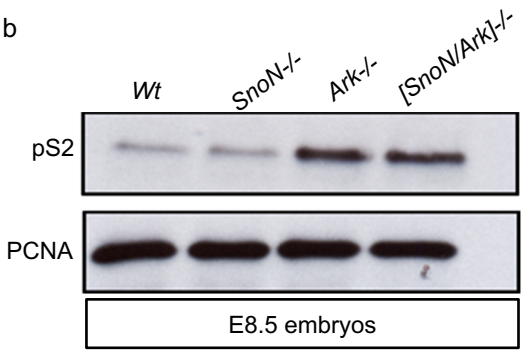

c

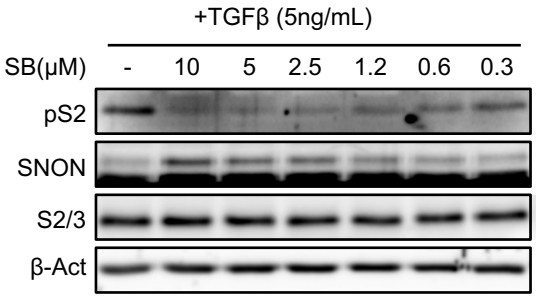

Extended Data Table 1

gene symbol	refseq_id	WT_18_T0_	WT_18_T3_	WT_18_T6_	WT_26_T0_	WT_26_T4_(	WT_26_T6_	A-/-_25_T0_	A-/-_25_T3_	A-/-_25_T6_	A-/-_39_T0_	A-/-_39_T3_	A-/-_39_T6_
Gal	NM_0013296	0.301309	9.89265	5.69885	0.185166	11.6717	7.28585	0.48687	1.59483	1.37061	0.190167	1.14273	0.949186
Ctla2b	NM_007797	0.031826	2.02704	1.78561	0.114925	1.57846	1.97079	0.164566	1.10102	1.64303	0.282756	1.1325	1.45263
Lefty1	NM_010094	0.02099	93.7814	40.8536	0.051595	111.231	40.7898	0.108531	70.4708	35.4317	0.127173	49.3926	27.7864
Col8a2	NM_199473	0.30886	6.06304	2.31302	0.090404	7.58336	0.767249	0.238712	3.02681	2.57071	0.587088	2.49049	1.9739
Exoc3l4	NM_0012894	0.463469	1.37623	1.17095	0.379759	1.22591	1.25135	1.02706	0.811566	1.39903	1.3372	1.0446	1.96305
Fam101a	NM_028443	0.369192	2.07987	2.14524	0.108821	2.31413	1.06605	0.378268	1.0108	0.895706	0.163632	0.680192	0.377045
Gsc	NM_010351	0.184819	7.47953	2.42119	0.100959	7.44442	1.78077	0.292003	4.77111	1.48255	0.342161	4.74768	1.09594
Lefty2	NM_177099	0.028331	47.8244	17.3232	0.069642	49.2998	21.7855	0.0651072	27.8549	19.4114	0.085827	21.008	12.9917
Adap2	NM_172133	0.452372	1.38907	1.11117	0.092667	1.76335	0.75439	0.292386	1.00817	1.46036	0.34261	1.23527	0.838274
Tspear	NM_0012870	0.675389	4.16243	3.04004	0.857531	5.07691	3.88416	1.12046	2.83146	2.81364	1.30594	1.99419	2.59179
Prkg2	NM_008926	0.690902	1.44866	3.38082	0.744901	1.65969	3.12072	2.29086	1.37017	4.76059	2.03351	1.92633	3.61747
Nfic	NM_008688	1.01057	11.6167	2.97874	0.828067	8.20672	4.49403	0.725747	4.31671	1.77947	1.70083	3.27053	2.24718
Utrn	NM_011682	1.41657	2.89986	3.94349	0.773813	2.99099	1.83736	1.62771	2.36777	2.49438	2.38413	1.71918	2.8
Zdhhc1	NM_175160	0.208425	1.33908	1.02392	0.170781	1.50303	0.834185	0.431083	1.16126	1.17442	0.29466	0.860027	0.617961
Cd40	NM_170704	1.88597	72.1271	30.8038	1.41979	71.523	26.7269	2.1088	40.4648	27.9824	2.69464	37.2064	30.378
Zbp1	NM_021394	0.112214	4.78397	4.83971	0.164604	4.0169	6.18825	0.03325	0.59483	1.75392	0.089545	0.870816	1.70653
Krt17	NM_010663	0.556111	5.08607	3.49692	0.692617	4.33546	3.31387	0.632609	1.90863	2.14125	0.628959	2.1867	1.91262
Sox15	NM_009235	0.94776	2.96427	2.02295	1.28537	3.12112	2.36169	1.71803	1.74804	2.4937	1.15508	1.66584	1.93794
Itpkb	NM_0010811	0.954906	8.0553	2.11005	0.774924	9.5778	1.71378	0.601228	3.93901	1.93867	1.29804	3.46279	0.891354
Gbp2b	NM_010259	0.488584	2.43029	4.36277	0.529859	2.28261	5.06441	0.990717	1.7454	4.25101	0.914205	2.17998	4.49493
Ddx42	NM_028074	0.404225	1.47311	1.41843	0.662432	1.68823	1.7334	1.1446	1.99478	1.69472	1.69109	1.75206	1.88334
Grm6	NM_173372	6.87761	15.5076	19.9037	3.223	20.1141	19.9663	4.87279	10.4236	18.6602	5.01104	8.47481	11.5333
Mkx	NM_177595	0.635827	8.30334	3.87292	0.672707	8.1071	4.25256	0.659279	3.50348	3.35132	0.641154	3.95242	3.81613
Smad7	NM_0010426	0.197742	11.3622	5.77114	0.235427	12.1969	6.49326	0.383227	8.46444	4.83225	0.330212	9.30182	4.35161
Zfp819	NM_028913	0.592375	3.37381	1.27725	0.647129	3.64	1.32712	0.939919	2.06494	1.00746	0.566998	1.76449	0.71668
Il15ra	NM_0012714	0.297189	1.11121	1.29561	0.1834	1.02077	1.07373	0.340362	0.7824	1.92293	0.310207	0.641509	1.54266
Has2	NM_008216	0.776619	5.17991	5.60576	0.680453	4.2187	5.33434	1.21928	3.26453	5.30757	1.07154	3.6581	5.08396
Tnfrsf13c	NM_028075	0.861422	2.67665	0.97073	0.75469	2.27261	0.42307	0.774268	1.19583	1.04154	1.05051	1.47864	1.22658
H2-M3	NM_013819	0.613734	2.4161	3.4673	0.460977	2.61663	4.60567	0.661134	1.33929	2.58166	0.413173	1.11726	1.85757
Slc6a15	NM_175328	1.08967	9.90436	11.5052	1.38642	9.55098	8.46426	1.24448	4.4528	7.40684	1.49691	6.46533	9.29688
Dync1h1	NM_030238	0.500346	1.01634	0.506883	0.450118	1.32242	0.942418	0.896406	1.20485	1.02948	1.00975	1.19225	0.834455
Mfsd4a	NM_0011146	0.784839	2.3576	1.55394	0.722833	3.07853	1.59475	0.989355	1.66945	1.90849	0.773316	1.55672	1.05777
Cxcl16	NM_023158	0.539064	1.37123	1.22226	0.407724	1.3335	1.33691	0.643234	1.24758	1.11958	1.17246	1.20779	1.29091
Pmepa1	NM_022995	0.09111	9.49651	2.59601	0.117313	9.58251	3.46917	0.0448669	3.71286	1.30633	0.279257	3.43165	1.34581
Slco4c1	NM_172658	0.399184	3.03895	0.952458	0.284222	2.60152	1.25581	0.646413	2.06629	1.56645	0.368978	2.01992	0.950896
Erap1	NM_030711	0.362278	1.66773	2.3023	0.290529	1.4347	3.06786	0.438417	0.86751	2.25307	0.280214	0.832562	1.63403
Wnt3	NM_009521	0.310701	4.61589	2.08427	0.289699	4.57302	2.6681	0.480118	3.95168	2.41478	0.400304	3.0816	2.08064

Mab21l3	NM_172295	0.657859	2.40489	1.35251	0.536723	2.30065	1.13584	0.746167	1.44699	1.22994	0.521663	1.15921	1.03967
Ptges	NM_022415	0.824138	3.64136	3.40544	0.695148	3.70857	3.47886	1.44135	3.13325	3.03466	0.905661	2.7064	2.67001
Nxph4	NM_183297	0.397603	1.52351	0.412359	0.361989	1.48529	0.270134	0.418793	1.00918	0.466747	0.401507	0.750616	0.16373
Ebf2	NM_010095	0.897553	5.30375	0.905487	1.29698	5.00714	0.956746	1.51959	2.86083	1.39221	0.572999	2.03962	0.3951
Steap2	NM_0011031	1.23014	5.443	4.29528	1.8203	4.41256	4.1934	1.92623	3.67012	3.90905	1.90959	3.68008	2.30879
Sphk1	NM_0011724	0.30765	1.44303	0.842072	0.351126	1.59004	1.19104	0.771699	2.24069	0.941559	0.68789	1.5602	0.952899
Tdgf1	NM_011562	13.875	280.108	225.288	16.5579	300.428	257.23	19.7601	210.065	213.589	23.4439	259.438	270.143
Skil	NM_0010390	10.9271	35.495	28.5567	11.1067	38.6448	28.2133	8.80796	15.743	14.1159	7.96846	16.2048	14.0175
Ctsw	NM_009985	0.397329	3.84549	3.94699	0.383046	3.87916	3.56018	0.502972	2.97913	3.76059	0.452463	2.41401	4.20972
Serpine1	NM_008871	1.81651	7.38099	7.02959	1.76237	7.14596	7.57009	3.92802	9.25159	13.2654	2.86968	6.55957	10.1933
Col2a1	NM_0011135	2.11376	4.49228	3.18655	1.42635	4.50128	2.96833	2.39149	3.84656	3.32119	2.45994	3.47416	3.75832
Clic5	NM_172621	0.60732	1.25044	1.26571	0.40996	1.08001	1.66667	0.861819	1.15364	1.17611	0.612661	0.824865	0.849881
Ctla2a	NM_0011457	0.189621	1.49297	2.54621	0.233059	1.3551	2.42434	0.408533	1.54952	1.74367	0.255311	1.03558	1.78033
Rin2	NM_028724	0.141551	2.10639	2.12093	0.318957	2.6209	1.84909	0.27447	1.97166	1.20471	0.285881	1.76083	1.9935
Nanog	NM_0012898	3.95282	79.9585	53.7743	3.44656	85.1311	48.1846	5.44098	69.8612	44.7091	4.97947	67.2092	49.4779
Socs1	NM_0012716	1.83886	5.04924	2.68185	1.22422	5.40392	2.87488	1.48566	3.71394	3.20422	1.68282	2.8942	2.17229
Ppp4r4	NM_028980	0.4102	3.31025	6.45651	0.299188	3.126	5.67563	0.282855	1.68905	4.01491	0.307769	1.53366	4.64102
Pnpla3	NM_054088	2.20438	6.91135	4.52046	2.66914	5.85959	5.01079	2.78754	3.91638	3.9392	2.91595	5.30967	3.49755
Timp4	NM_080639	0.504536	7.38873	4.80467	0.826818	6.35392	5.95439	0.618757	3.87062	3.64477	0.764234	5.58149	4.89044
Parp9	NM_030253	1.31365	3.4264	7.01782	1.16093	3.41509	9.01404	1.55396	2.67633	5.70603	1.54242	2.55182	6.16855
Ccl25	NR_033527	19.0452	38.4003	36.8865	13.9567	37.3995	32.26	31.8793	41.7931	50.7729	28.9287	44.8634	52.5105
Fhl2	NM_010212	1.30537	5.21965	5.61122	1.146	5.88343	5.36446	2.29008	6.20803	9.24901	1.55358	4.52637	7.63694
Fgd6	NM_053072	0.65928	1.39811	0.83561	0.725776	1.48345	0.754947	0.746161	1.0432	0.875189	1.04771	1.24864	0.859186
Id1	NM_010495	12.2322	41.0422	14.5241	11.3687	46.3757	10.1394	47.4557	103.891	21.869	35.9658	87.6554	23.0035
Kcnmb4os2	NR_130644	1.22189	3.1168	2.9148	0.601778	2.48494	1.93169	1.22354	2.47127	2.15582	1.38336	2.96582	2.09402
Fam214a	NM_0011132	3.1502	8.14698	2.48564	2.56024	8.94318	4.45125	1.47461	4.31885	3.32032	3.3187	2.88918	3.95702
Tagln3	NM_019754	0.885067	2.91329	2.88932	0.842179	2.55968	2.34885	1.20562	2.79966	1.91038	1.23973	2.04432	2.11624
Herc6	NM_025992	2.45085	5.38754	8.78126	2.3744	4.953	11.0248	2.05158	3.2965	9.58023	3.33932	3.63183	8.1147
Sptan1	NM_0011776	0.648165	2.14338	1.91052	0.763451	1.65805	1.93661	1.43136	2.70848	1.56932	1.79995	2.80235	2.6424
Lgr4	NM_172671	0.274688	1.55717	1.02557	0.315105	1.87379	0.916156	0.331411	1.34679	0.709403	0.443815	1.46681	0.977305
Trim34a	NM_030684	0.897621	2.59087	3.1248	1.09009	3.27933	2.73522	1.11868	2.41366	3.36125	2.04809	3.24755	4.19625
Hecw2	NM_0010018	0.932703	2.88829	3.302	1.03049	2.67371	2.70144	1.1434	2.6016	2.24773	1.32413	1.82133	2.4426
Tmem17	NM_153596	6.05101	18.1505	16.2891	5.82476	19.2483	15.2593	7.33446	17.1858	17.0652	9.6624	16.747	19.618
Dtx3l	NM_0010133	0.604163	1.78737	1.28699	0.406379	2.30853	1.29487	0.51412	1.25121	0.987045	0.376359	1.1878	0.776582
Nefl	NM_010910	5.32485	13.0672	15.2899	4.41259	11.0256	12.7575	7.16525	9.89302	11.6036	4.97054	9.0766	11.6094
Clca4a	NM_207208	1.27722	9.18266	15.9424	2.1454	9.28571	15.0529	1.28581	6.0026	14.3515	2.67061	7.47146	16.8135
Casq1	NM_009813	0.943247	2.04231	1.85353	1.06271	2.2597	1.79146	1.25319	1.708	1.66092	1.07157	1.52632	2.214
Psmb10	NM_013640	19.2694	45.9379	57.8198	17.5171	41.5821	60.2537	20.1414	35.1539	54.4991	26.6352	35.9025	54.7763

Hspb2	NM_024441	2.87641	6.25495	6.01116	2.91805	6.76297	5.12673	6.76765	10.4806	9.80827	5.9015	8.20076	7.37762
Plekha2	NM_031257	3.25944	14.2574	11.2879	3.45934	14.8046	12.0282	5.15204	14.4653	14.4432	4.76934	13.9135	13.8979
Fgf17	NM_008004	0.605182	1.37228	2.0613	0.694227	1.5137	2.60155	1.25169	1.73087	2.39176	0.957426	1.4934	1.91392
Nfkbid	NM_172142	0.454897	1.47357	1.40469	0.372735	1.13991	1.22821	0.616037	1.08621	0.686576	0.393739	0.946408	2.3121
Junb	NM_008416	3.22879	17.445	11.9866	2.99414	17.5976	11.1988	5.04853	18.8297	11.6886	3.88525	14.5243	11.4647
Gng11	NM_025331	1.94506	6.73828	10.2348	2.93958	6.10761	10.668	4.13468	7.85083	11.2135	3.44817	6.18991	9.29111
Cnpy1	NM_0013105	0.437632	5.31618	2.32672	0.463241	4.59061	2.06516	0.318361	2.31066	1.23152	0.276688	2.07829	1.17504
Spats2l	NM_144882	0.687548	1.77208	2.78445	0.462081	2.05757	3.37788	1.08619	1.88307	3.92726	0.74976	2.24121	2.91176
Apobec2	NM_009694	0.819824	3.25858	2.7498	0.926553	4.3252	3.48863	1.60793	3.59117	4.77877	1.17044	4.21998	3.77177
Lypd1	NM_0013110	0.719635	2.54161	2.23902	0.659855	1.75322	1.9049	0.590639	1.39378	1.32751	0.761305	1.39322	1.93044
Smad6	NM_008542	0.12521	1.15934	0.356763	0.235968	1.03715	0.473288	0.431615	1.50685	0.293967	0.202302	1.17007	0.352672
Kirrel2	NM_172898	0.050203	1.1621	0.715224	0.071987	1.10077	0.962783	0.0973447	1.02094	0.928201	0.06337	0.990071	1.09775
Miat	NR_033657	0.509769	2.08685	1.12578	0.633803	1.80966	1.10549	0.564723	1.65912	0.948929	0.811451	1.44687	1.19854
Zfp423	NM_033327	0.92075	3.50324	2.01016	0.82443	3.50677	2.07697	1.04092	2.60219	1.91429	0.8759	2.60739	1.92243
Coch	NM_0011988	1.93927	10.3667	3.3595	2.45669	9.69781	3.90065	4.85979	13.7762	6.60489	4.01969	14.0129	4.63385
Chst15	NM_029935	0.501998	6.12574	2.28551	0.347602	6.67653	2.51537	0.402149	4.0969	2.12478	0.392689	4.39335	2.23256
Pitx2	NM_0012870	0.562444	59.3012	37.9465	0.378959	62.4512	34.8986	0.744296	48.7914	30.8	0.433422	51.4238	40.2304
Cntfr	NM_0011360	1.67262	3.8644	2.31809	1.47895	3.67025	2.36985	2.10041	3.0811	2.10078	1.75557	3.18522	2.06803
Ppp1r36	NM_0011631	0.294637	2.58131	1.28954	0.351158	2.08818	1.19114	0.184665	1.13419	0.723193	0.243433	0.975212	0.675031
Nodal	NM_013611	7.98458	57.5156	63.441	7.36222	56.567	61.0901	8.72146	40.7992	42.6646	7.69382	43.5244	51.8535
Tcf15	NM_009328	10.4606	50.5186	23.0266	9.2283	44.7183	23.2188	9.14046	32.898	22.249	9.2383	28.8407	19.0735
Rhob	NM_007483	10.9547	26.7477	19.5212	9.02163	26.8441	17.952	13.5806	26.7348	20.0638	13.9785	25.427	20.9944
Bambi	NM_026505	6.77547	15.569	14.2037	7.18384	15.1024	12.5992	10.5726	17.0001	15.0749	11.3525	16.7204	17.1357
Parp10,Plec	NM_0011635	1.6532	4.48167	4.67359	1.74404	3.92871	4.93412	2.08599	3.24964	3.59836	1.76428	3.39308	2.86715
Psme2	NM_011190	55.2172	150.015	222.384	55.0561	138.089	214.899	59.5933	117.952	179.447	72.9648	123.036	212.806
Dkk1	NM_010051	0.15884	3.40882	1.85047	0.223116	2.32185	1.86682	0.293327	2.90782	3.2764	0.229141	2.86402	2.48927
Irf1	NM_0011593	3.98559	76.875	45.2556	3.60987	85.2543	46.9323	4.2965	65.2901	37.8058	3.75993	56.3291	36.8027
Pik3ip1	NM_178149	1.41147	6.55085	3.83189	1.30674	7.15491	4.06423	1.86231	5.48582	3.17387	1.27394	5.33024	3.05268
Cx3cl1	NM_009142	0.380528	2.13662	1.01481	0.187079	2.48983	1.11203	0.356042	2.36245	1.19971	0.285453	1.91324	0.950934
Panct2	NR_131964	0.279958	2.86689	1.46837	0.336136	2.97049	1.42745	0.500375	2.98225	1.59982	0.423832	3.18173	1.86828
Gm14005	NR_028590	2.96627	8.51912	11.0191	2.64617	9.64296	8.37072	5.39975	11.8201	13.2295	4.95571	12.1287	13.2975
Dact3	NM_0010816	1.73455	5.64871	3.481	1.79422	5.3467	3.62428	2.02488	4.33175	2.67159	1.88823	4.34453	3.19143
Trh	NM_009426	13.0533	73.7802	97.784	10.9787	65.6667	87.0471	17.1416	70.0855	100.291	13.6232	57.4719	92.1473
Nxn	NM_008750	19.6277	54.6674	49.9209	17.845	52.2622	53.1287	15.4158	30.882	40.3562	13.2334	27.7859	34.9688
Radil	NM_178702	0.526607	2.69195	2.28767	0.292919	2.64475	2.61923	0.484543	1.79989	2.53374	0.324418	2.1166	2.47389
Prkd2	NM_178900	0.725773	1.65623	1.09259	0.865614	1.84072	1.35492	0.967959	1.57962	1.16732	0.816239	1.28181	1.19825
Fgf3	NM_008007	1.42167	3.94009	3.0963	1.20372	3.69446	2.58156	1.34769	2.77233	1.72453	1.53134	3.36447	1.65092
Abcg2	NM_011920	29.7662	88.0869	107.092	27.6785	79.3663	98.1564	29.982	62.7143	95.1259	32.9048	70.9391	102.855

Cdh6	NM_007666	0.590997	1.25636	1.21482	0.477882	1.00788	1.14118	0.797477	1.15248	1.05892	0.526126	0.868245	0.818484
Rab19	NM_011226	1.11144	3.42334	4.78304	1.51176	3.37928	6.32653	1.36011	1.80821	3.41837	0.830541	2.13121	4.02028
Gm15417	NR_040403	2.45273	5.74517	5.91003	2.39882	5.90047	4.68175	2.88734	5.12216	4.78992	3.17419	5.56203	4.40929
Pycr2	NM_133705	42.1748	196.726	158.516	38.38	192.002	174.435	41.9345	153.716	158.964	44.6803	156.345	174.138
Mfap4	NM_029568	2.52537	7.81538	6.11613	2.33416	6.85444	6.78938	2.39258	4.67624	5.06213	1.24862	3.15523	2.99781
Sfn	NM_018754	3.31141	13.2777	8.54386	3.50746	13.4851	10.0268	4.22259	13.7399	10.8401	3.83327	9.89995	9.41889
Dok2	NM_010071	3.02323	10.1218	10.7898	3.43606	11.95	10.7023	3.19902	8.49958	8.08047	3.12967	7.5878	11.182
Gm15867	NR_131748	0.189811	1.31513	1.11897	0.492506	1.079	0.66824	0.29989	1.1633	1.5226	0.44724	1.30536	1.50072
Pdlim3	NM_016798	3.43725	8.63893	10.9483	3.11096	8.73527	11.9387	4.02701	7.3099	9.99517	3.35756	7.22517	10.1245
Mpc1	NM_018819	15.109	40.0859	26.2412	17.5489	36.3881	24.4328	18.5447	33.7859	29.0234	22.3466	38.2167	31.3728
Stx3	NM_0010253	18.5157	48.4691	53.7859	18.057	44.5292	56.1264	16.2585	31.6431	46.1631	20.3795	37.9778	53.7422
Mir9-3hg	NR_040314	1.25942	2.57227	0.913724	1.00436	2.53972	0.921418	1.19223	1.46157	1.548	0.978653	2.15383	0.828313
Krt42	NM_212483	0.854938	3.39733	3.16235	1.17441	3.35707	3.32669	0.888462	2.21356	2.45	0.863331	2.28876	2.31115
Lmo2	NM_0011423	0.401311	2.10354	2.0495	0.641758	2.15326	2.15258	0.468057	1.18021	1.55861	0.378002	1.49293	1.50761
Six2	NM_011380	0.819342	2.82645	1.29178	1.06168	2.58104	1.54642	1.19872	2.54793	1.81181	1.07753	2.49749	1.15814
Zfp870	NM_207245	0.848176	2.02011	1.38892	0.709461	1.85974	1.51267	0.670034	1.2208	0.891958	0.678064	1.32959	1.20499
Syt13	NM_030725	2.65262	10.2799	8.87961	2.13539	9.43296	8.96102	2.53464	7.83044	8.50044	2.02075	6.51762	7.79577
Ctgf	NM_010217	6.65183	22.3851	21.0103	5.93515	22.3855	21.4958	9.42559	25.5972	28.8122	7.59138	20.8036	24.6846
Aldh1b1	NM_028270	1.76961	3.58754	1.75365	1.28691	3.91934	1.36547	1.38335	2.34856	1.23596	0.974442	2.12703	1.1898
1110037F02I	NM_0010811	0.559263	1.8494	1.02048	0.752842	1.67394	1.24353	0.895078	1.82508	1.40683	1.04883	2.32708	1.65816
Avpi1	NM_027106	44.0682	106.622	88.3415	40.475	101.647	76.8091	50.0119	107.801	82.5406	67.1997	110.606	109.774
Nedd9	NM_0011113	1.03481	3.44705	1.81119	1.21683	3.04797	2.27713	1.36056	3.25313	2.41069	1.57683	3.33766	2.403
Steap1	NM_027399	6.38516	15.1233	14.5238	6.73697	15.0303	16.5313	7.81425	14.0352	15.6756	7.30167	12.8445	16.5109
Rps6kl1	NM_146244	1.86834	7.10777	6.79042	1.61217	6.65442	8.62102	1.73834	5.74831	6.1139	1.51936	4.29411	5.29432
Igsf11	NM_170599	0.506952	1.04041	2.38185	0.200394	1.28149	2.28455	0.608473	1.50506	1.67861	0.269919	1.10449	1.05398
Mup6	NM_0010812	7.031	23.0696	36.7066	8.94901	23.2067	37.0421	6.91061	18.414	34.018	12.227	23.5425	44.5393
Mb21d2	NM_177718	4.48131	10.8491	9.22452	4.80622	10.0486	9.44137	5.35318	8.84016	8.88576	5.54686	10.4034	10.4978
Homer3	NM_0011461	8.51853	20.0667	16.8077	7.0828	16.046	14.7205	9.82977	16.8344	13.9449	7.35711	14.0646	14.631
Lgr4	NM_172671	7.21139	24.0115	17.3459	6.75983	24.4141	18.2935	8.28253	21.5198	19.4599	7.00862	20.0323	15.6246
Kazn	NM_0011096	0.900672	2.15805	1.46766	0.668391	2.3171	1.72682	0.866703	2.05637	1.36049	0.911429	2.05209	1.20958
Irgm1	NM_008326	0.342823	5.80374	3.62634	0.281093	5.45	4.32928	0.251043	4.3469	3.63559	0.363448	4.12411	3.20467
Pcolce2	NM_029620	7.5946	16.0068	13.6824	7.00215	14.1664	14.0017	6.84934	11.6723	12.5197	6.39325	9.97542	10.4127
Mdfi	NM_010783	8.14743	25.8088	13.0969	7.43034	24.8124	14.45	7.86349	19.2484	13.6456	7.56159	20.486	15.729
Relt	NM_177073	1.69514	5.47778	3.41366	1.45988	5.01333	3.27271	1.74249	4.82558	2.6628	1.67762	4.25333	2.88183
Notch3	NM_008716	1.05644	4.4421	4.4649	0.849112	4.86462	4.74285	0.96255	3.79673	3.76307	0.785859	3.127	3.46101
Bcar3	NM_013867	2.74729	24.9068	15.656	2.55827	25.175	18.275	2.74169	22.3539	14.3865	2.71765	18.8377	13.7737
Prrx2	NM_009116	3.11648	8.96375	6.36792	2.4858	7.95539	5.24313	5.98943	12.2622	9.55078	4.59528	12.9533	8.91296
Rnd3	NM_028810	18.7578	42.4265	38.8494	19.5174	42.9093	41.7987	23.4656	41.0781	46.7169	25.4283	46.8712	49.6464

Btg2	NM_007570	9.01833	20.6619	9.88989	7.74535	19.6681	9.01787	8.38834	16.3835	8.92215	7.44286	14.5414	7.72612
Nxph3	NM_130858	0.495301	1.68042	0.420285	0.295158	1.57966	0.525623	0.388039	1.42998	0.581434	0.38649	1.31151	0.43388
Tppp3	NM_026481	3.53584	15.4857	14.9596	4.06072	17.1942	12.671	4.59389	17.4111	13.067	6.27818	20.0489	14.7155
C130071C03I	NR_015561	0.296566	1.20486	0.509922	0.328053	1.19937	0.741845	0.357807	1.20621	0.57443	0.389321	1.15174	0.615503
Hey1	NM_010423	1.07244	2.61389	1.83251	0.776854	2.68089	2.15994	1.52696	2.21687	1.73331	0.878927	2.98031	1.86632
Unc5b	NM_029770	2.1757	10.5298	5.65503	2.02831	10.8932	5.75091	2.42983	10.1058	5.32311	2.22508	9.43697	5.06842
Igtp,Irgm2	NM_018738	2.18732	4.48413	3.65279	2.22257	5.15513	4.62806	1.92617	3.60189	3.63713	1.63993	2.83045	2.9548
Tmem119	NM_146162	0.483875	2.66683	0.950839	0.46256	2.92354	0.96831	0.430897	2.22865	0.852032	0.407188	1.85959	1.00425
Platr8	NR_033473	1.8247	4.66493	4.74568	1.84692	5.64832	4.41522	3.2375	6.81751	4.03203	2.27617	5.73162	2.86414
Trim34b	NM_0012439	0.56013	1.71996	0.997494	0.803183	1.77401	1.55682	0.633559	1.36535	1.35617	0.618656	1.35957	1.73857
Zfp946	NM_198003	5.37696	15.823	16.2514	6.40525	15.0257	16.4691	4.82762	11.4119	15.3559	8.26133	16.572	21.561
Nkx6-2	NM_183248	2.84058	6.38847	6.55786	1.98482	6.30053	6.18044	2.58314	6.03933	5.03253	2.46371	5.3297	5.01189
Pkdcc	NM_134117	4.63022	12.8644	12.7435	3.76016	13.5097	13.1365	5.68345	14.1772	16.1611	5.49427	15.4907	15.5002
Pde4b	NM_0011779	0.808071	3.26848	3.48733	0.750579	3.01661	3.02964	0.666832	1.7842	3.36221	0.604623	2.45521	3.77366
Lrrc2	NM_028838	1.1401	2.52486	2.21211	1.0219	2.85821	2.20181	0.877736	2.09183	1.98433	1.00735	1.82577	1.57346
1700057H15	NR_040774	0.748667	2.12205	1.10338	0.920169	2.00634	0.62425	0.806488	1.45994	1.53801	0.756016	1.81719	1.10986
Cacna1g	NM_0011778	0.850654	7.39594	3.92038	1.11049	8.5047	4.46207	0.715599	6.18275	2.51363	1.16677	5.9615	3.01782
Msx2	NM_013601	0.678747	1.77958	1.28376	0.472732	1.53785	0.98098	1.16987	2.70391	1.85252	0.97671	2.57419	1.81118
Dok5	NM_029761	0.521039	1.70248	2.23971	0.462509	1.22707	2.05157	0.374187	0.798329	2.34465	0.350769	1.00121	1.57701
Crlf1	NM_018827	2.78933	10.819	10.0689	2.27731	10.103	9.06792	2.65524	8.47013	8.84173	1.90345	7.29694	8.23668
Kif26a	NM_0010976	0.808401	1.91867	0.794277	0.873879	1.95049	0.747158	0.74286	1.51402	0.705427	0.899938	1.67259	0.840161
Trim6	NM_0010136	2.12058	4.9178	2.65176	2.36941	6.38741	3.00054	1.99362	4.94081	5.205	3.69878	6.55092	2.85787
Kbtbd3	NM_026962	2.47347	6.18086	5.97665	2.72101	7.08988	5.1245	2.94012	6.95768	6.32599	4.31941	8.46464	8.43794
Plekhh1	NM_181073	0.929214	1.90297	1.10144	0.861404	1.94274	0.988051	0.874851	1.47057	1.08568	0.660356	1.30004	1.35073
Pde1b	NM_008800	1.00492	3.29703	2.56062	0.542911	3.28227	2.30811	0.732791	2.64568	2.19083	0.591029	2.5598	1.99724
Nespas	NR_002846	1.03137	2.08798	1.71593	0.779441	1.65037	1.36589	1.05126	1.53759	1.27925	0.815073	1.6866	1.36363
Pth1r	NM_0010839	0.843698	2.44705	0.929381	0.614662	2.59598	1.15562	1.1506	2.73098	1.57001	0.68287	2.54962	1.29268
Tnfaip6	NM_009398	0.909185	3.77565	3.59397	0.987522	3.72946	3.1264	1.89503	7.18609	5.88252	1.94298	5.85061	5.48532
Runx1	NM_009821	1.09983	2.5023	1.8065	0.399267	3.42325	3.65475	1.09937	4.00112	2.0737	0.576252	3.28511	2.16615
Ubr7	NM_025666	51.9925	144.464	127.229	49.0124	147.54	126.657	49.9152	119.86	123.974	51.047	131.937	130.583
Efna3	NM_010108	1.30428	3.80203	1.34822	0.871107	4.85718	1.93922	1.2044	4.54822	1.60402	1.27009	4.50291	1.91101
Papolb	NM_019943	0.312271	1.76395	1.04448	0.391971	1.89708	0.775589	0.326368	1.33264	0.935935	0.261662	1.2982	0.709162
Fermt1	NM_198029	0.385989	1.26216	1.27098	0.362832	1.1945	1.377	0.276531	0.765179	0.949246	0.2333	0.677595	0.875258
Fat1	NM_0010812	4.73375	13.5995	9.99964	5.25566	13.522	9.99971	6.34218	14.9884	11.6141	4.98684	11.7158	8.67329
Fam25c	NM_183278	19.6348	49.2816	44.7768	15.7274	48.1506	42.9726	19.8784	52.3374	52.1702	24.2645	53.1242	52.7759
Arl4a	NM_007487	93.2095	241.082	211.314	95.0883	228.516	197.921	98.1099	230.455	197.801	118.51	234.529	227.353
Lama5	NM_0010811	1.65631	7.11897	4.41595	1.93912	7.6573	4.35696	1.86044	6.88209	4.07982	1.68391	5.85662	3.94111
Yaf2	NR_028315	9.90559	28.0411	23.4499	10.9475	26.3159	22.704	12.1679	27.0425	24.9587	13.2182	30.9	30.6974

S100a10	NM_009112	128.409	264.703	281.956	132.73	272.495	256.456	201.629	407.468	367.933	243.364	383.281	424.685
Slc7a7	NM_011405	36.6397	84.2148	85.0234	38.1061	77.194	92.4098	30.9626	58.7557	73.9918	30.8786	58.7152	67.9434
Nfic	NM_008688	1.74575	5.20568	1.58376	1.68893	4.04038	1.97687	1.93094	3.22062	1.29973	1.21491	3.75783	1.61377
Eomes	NM_010136	1.18592	5.48914	4.00385	1.20438	4.99856	4.03658	1.11013	4.11732	3.33213	0.900897	3.67741	2.99994
Pdlim4	NM_019417	0.456595	1.12174	1.34585	0.395859	1.58912	0.979033	0.562164	1.92615	1.07201	0.562471	1.3062	1.15567
Nectin4	NM_027893	0.420467	1.25731	0.54687	0.429637	1.3799	0.545299	0.290581	0.902099	0.455186	0.356589	0.858398	0.373918
Mrc2	NM_008626	0.605485	1.637	1.12574	0.561003	1.94716	1.36184	0.626158	1.62967	1.21926	0.573803	1.6675	1.15998
Dok1	NM_0012917	5.20029	12.0674	8.48445	4.431	11.8727	8.04994	5.37806	11.8792	9.29812	5.46802	12.3887	10.0043
Sertad4	NM_0011777	2.94227	10.5338	9.65874	2.9672	11.0663	10.0211	2.48472	8.31168	8.19009	2.5538	8.16864	7.64403
Irak2	NM_172161	1.30834	5.4189	4.28029	1.31847	5.6365	4.38039	2.08723	8.78521	6.31473	2.46701	8.24584	6.75847
Card10	NM_130859	0.988089	2.26158	1.66134	0.695593	2.25128	2.0191	1.15735	2.86117	1.80523	0.857256	2.13654	1.50605
Endod1	NM_028013	0.600349	1.88345	1.20997	0.636969	1.80013	1.15519	0.729628	2.01552	1.5631	0.551837	1.44785	1.18665
Hes1	NM_008235	4.72298	21.2382	16.8501	4.09454	23.1689	18.1924	4.53121	18.8629	15.269	3.88252	19.899	15.4056
Msx1	NM_010835	2.34499	17.8448	5.96542	2.0555	17.821	6.40648	2.94516	18.6155	7.76754	2.00088	17.1638	7.57246
Kras	NM_021284	10.266	24.2726	16.9592	10.0246	23.8408	17.582	10.3242	21.181	18.1208	9.3519	21.5232	18.3834
Thbs1	NM_0013139	1.48261	5.67241	4.47535	1.21021	5.25187	4.5438	1.70035	6.26291	6.23382	1.29223	4.9396	5.86664
Cpt1a	NM_013495	1.4929	5.33466	2.26606	1.02537	6.21886	3.32895	0.854255	3.7169	2.55693	0.872327	3.96314	1.80569
Lax1	NM_0011596	0.758729	2.71159	1.653	0.810901	2.89324	1.50367	0.824434	3.67593	1.66517	1.79885	3.96348	1.56491
Pxdc1	NM_025831	2.64308	11.8682	10.1395	2.93497	10.8281	7.72318	2.63265	7.99053	10.8901	1.68686	8.02567	9.13248
Dmtn	NM_0012526	0.980323	3.2199	1.90834	1.105	3.24825	1.71437	1.3803	3.48166	1.78852	0.672975	2.32274	1.15498
Ap3b2	NM_021492	0.540465	1.18541	1.38445	0.569377	1.31671	1.50216	0.615475	1.09695	1.37087	0.331361	0.843324	1.45935
Il17rd	NM_134437	1.55254	4.00021	3.83195	1.39197	4.39635	4.23173	1.32503	3.79853	3.77272	1.24968	3.30872	3.5135
Sema3f	NM_011349	0.860605	1.72224	1.33961	0.83118	1.85504	1.38075	0.859589	1.61013	1.14965	0.742596	1.63475	1.37961
Rnf11	NM_013876	8.80517	17.7477	16.6784	8.67096	17.5923	16.1454	8.73852	18.0196	16.8214	9.89851	18.2591	19.4904
Zmiz1	NM_183208	0.939801	2.79921	1.50914	0.845769	3.20399	1.32714	1.00892	3.13245	1.61883	0.889175	3.06882	1.81268
Tle3	NM_009389	3.6028	7.70373	3.38907	2.92651	9.03765	3.57082	3.48375	8.68119	3.47532	3.06938	7.974	3.58165
Nav1	NM_173437	1.61618	4.1193	2.00896	1.44097	3.03029	2.13812	1.36666	3.19612	1.95584	1.33305	2.94845	1.92888
Tbc1d9	NM_0011113	0.707254	1.90299	0.983774	0.540364	2.67384	0.958107	0.700759	2.9572	1.40076	0.675509	2.21299	1.36243
Cthrc1	NM_026778	9.36431	19.4532	22.5593	8.45994	18.3974	23.8915	6.5181	15.0168	20.9638	8.15298	15.4808	21.4906
Mmp25	NM_0010333	1.5638	5.59246	5.11484	1.43309	5.80831	5.62745	1.15851	3.96663	3.88888	1.05277	4.34509	3.98577
Nuak1	NM_0010043	0.671403	2.29131	2.16668	0.621275	2.26179	1.95617	0.86292	3.18611	2.52755	0.695528	2.28995	2.26521
Ncor2	NM_0012539	2.08287	4.31905	3.27071	2.26282	4.64078	2.96334	2.18693	4.46534	2.92003	2.15984	4.45591	3.00621
Cxxc5	NM_133687	9.58335	19.3478	12.5177	7.84663	19.4038	11.955	9.67464	20.7708	11.7691	8.49347	20.0595	11.7734
Cpeb1	NM_0012525	0.557026	1.22094	1.60302	0.638015	1.43287	1.28663	0.657767	1.30093	2.02608	0.516336	1.28674	1.68102
Snhg9	NR_027900	29.7743	61.707	50.0149	31.4795	87.0456	45.9153	29.7976	84.5504	56.3743	56.2536	116.563	78.311
Atp1b2	NM_013415	0.599138	1.31721	0.803758	0.679741	1.4372	0.883855	0.804281	1.69475	0.784481	0.605019	1.38433	0.631982
Whrn	NM_0010087	1.28372	2.98047	2.32644	1.26404	2.7924	2.64564	1.14433	2.25716	1.64309	0.91088	2.42003	1.62937
Ago1	NM_0013171	2.31317	6.51648	4.79783	2.28601	6.76925	4.89793	2.13162	5.61368	3.83663	1.51347	4.96327	3.71188

Camk2n1	NM_025451	2.08228	6.48927	1.57176	2.1165	5.76052	1.579	1.56176	4.61839	1.63648	1.37553	4.20991	1.02867
Tcirg1	NM_0011360	0.932486	3.35634	1.81851	0.78387	3.13577	1.76071	0.715537	2.69272	1.43954	0.696557	2.84291	1.66607
Epb41l1	NM_013510	0.7644	2.60771	2.12366	1.00025	2.02535	1.87312	0.806007	2.38748	1.19759	1.04246	2.77114	1.91373
Itga5	NM_010577	2.16227	4.83519	3.15365	1.79625	4.83403	3.11095	2.74032	6.51136	4.55838	1.91906	5.24835	3.62694
Bhlhe40	NM_011498	0.450563	1.72356	2.32142	0.450225	1.59567	2.12584	0.61558	1.91032	2.39948	0.388403	1.77381	2.28076
Foxp4	NM_0011108	3.31912	6.7766	3.71069	2.31723	7.59518	3.88315	2.65463	7.05373	2.72987	2.10787	6.09111	2.66328
Jag1	NM_013822	0.671902	1.9967	1.16234	0.569369	1.41028	1.04706	0.633475	1.683	1.05166	0.504525	1.52633	0.868361
Rem2	NM_080726	0.544227	1.12396	1.11403	0.436099	1.03731	1.41016	0.53842	0.848097	1.03257	0.411	1.26373	1.66468
Irf2bpl	NM_145836	4.58893	10.8037	6.74094	3.88955	10.7546	6.55703	4.46684	11.6521	6.35837	4.25415	11.7775	6.64673
Epha2	NM_010139	2.79911	14.3277	12.7364	2.22473	14.3456	12.3148	2.09602	12.8853	10.1682	1.87538	11.289	10.3294
Agrn	NM_021604	3.68072	8.89625	7.28749	4.29034	9.73661	7.85968	4.162	10.6033	7.36426	3.85689	9.33441	7.61778
Chd9	NM_177224	4.27598	9.16509	7.80629	4.56325	9.4187	7.86699	3.49571	8.75585	6.74941	3.58086	7.12465	6.19929
Map2k4	NM_0013163	2.3137	7.15422	6.40649	2.92989	6.55916	5.8465	2.71897	9.84402	7.40742	4.03562	8.42385	9.35439
Ccdc85a	NM_181577	1.55763	3.85304	2.92517	1.25362	3.00643	2.26381	1.27813	3.41135	3.40645	1.11298	2.87251	2.81764
Zfhx3	NM_007496	3.81068	9.51877	4.84723	4.26846	10.8046	4.3722	3.75142	10.1833	5.30742	3.24303	8.81635	4.4441
Lrrn4	NM_177303	1.41771	3.15913	2.75083	1.37352	3.53646	2.60709	1.42155	3.04033	2.47021	1.17952	3.62508	2.72294
Gm15706	NR_045598	0.610117	1.7151	1.95958	0.844172	1.83425	1.90911	0.807477	1.76873	1.66182	0.616704	2.01825	2.11002
Tmem63a	NM_144794	0.15667	1.85468	1.08389	0.231073	1.89278	1.39346	0.180021	1.55149	1.1638	0.105471	1.48585	0.884714
Trim47	NM_0012050	0.643872	2.11742	1.21474	0.506571	2.2064	1.20282	0.531486	2.4949	0.967659	0.494114	1.96942	0.992393
Sh3pxd2a	NM_008018	1.92741	5.16217	2.78195	2.3669	5.45451	3.18142	2.30711	7.95423	3.48909	2.59193	6.03228	2.36964
Gm16386	NR_030709	1.19307	2.57652	3.01428	1.48965	2.98967	2.71596	1.22401	3.29199	3.06786	1.89323	4.068	4.12688
Mllt6	NM_139311	0.735042	1.7467	1.1979	0.6527	1.79774	1.20146	0.648992	1.937	0.746687	0.573013	1.74022	0.84352
Fgf15	NM_008003	1.06288	13.9662	8.99268	0.677375	14.1365	8.11848	0.559765	9.43125	6.83936	0.357773	8.31293	5.19388
Fzd4	NM_008055	0.56284	1.70361	1.40352	0.516547	1.29787	0.813071	0.785801	1.34871	1.01617	0.394741	1.95267	1.19577
Edn1	NM_010104	0.428122	1.71506	2.32194	0.434988	1.25162	1.31367	0.59032	2.53798	3.4175	0.536083	2.14066	3.09719
Gse1	NM_198671	1.81401	4.64159	3.51504	1.92311	5.59555	3.31426	1.96535	6.19619	3.02828	1.39511	4.93484	2.75356
Nrarp	NM_025980	2.06781	7.06334	2.57866	1.30333	5.96775	3.2715	1.30223	6.02635	2.52076	1.04405	5.40514	1.76851
Lzts1	NM_199364	1.56826	3.23304	3.83774	1.69879	4.3823	3.26689	1.0789	2.12494	2.36385	0.459139	1.79155	2.08761
Bmpr2	NM_007561	2.05186	4.86672	3.23731	1.90771	5.03867	3.02343	2.00556	5.36733	5.19036	1.47838	5.42519	3.06629
Tbx3	NM_011535	1.5167	3.83349	2.39045	0.655665	4.48431	1.0497	0.493388	3.77273	2.48705	1.09363	5.43874	2.17601
Pdgfb	NM_011057	0.418682	3.46743	2.0801	0.529958	2.99701	1.43711	0.210024	2.39491	1.51745	0.282163	2.69393	1.76146
Cbln4	NM_175631	0.47797	1.72927	2.16482	0.42985	1.54504	2.31995	0.140651	1.03924	1.61484	0.317851	1.16015	1.348
T	NM_009309	0.383501	2.10844	3.93727	0.496742	1.95387	3.65809	0.145134	1.4556	2.64447	0.378694	1.89654	4.14447
Mafb	NM_010658	0.414879	2.79711	1.45158	0.74214	2.21235	1.13129	0.282065	1.58468	1.07413	0.18156	1.94538	0.744864
Gata4	NM_008092	0.745822	2.24336	0.478218	0.879517	2.82786	0.773617	0.188194	1.57141	0.699541	0.762483	1.95403	0.485598

Primers used in Methods

In situ probe

SnoN exon-1 Forward	5'-AAGCTGAACGGCATGGAG-3'
SnoN exon-1 Reverse	5'-GAGTAATACGACTCACTATAGGGATGACGAACGTCTGGGGA-3'

Quantitative RT-PCR

β-Actin Forward	5'-TGGCTCCTAGCACCATGA-3'
β-Actin Reverse	5'-CCACCGATCCACACAGAG-3'
Smad7 Forward	5'-GGCCGGATCTCAGGCATTC-3'
Smad7 Reverse	5'-TTGGGTATCTGGAGTAAGGAGG-3'
Lefty1 Forward	5'-TGTGTGTGCTCTTTGCTTCC-3'
Lefty1 Reverse	5'-GGGGATTCTGTCCTTGGTTT-3'
Lefty2 Forward	5'-GATGGCTCCAATCGCACTG-3'
Lefty2 Reverse	5'-GTGGATGGACACGAGCCTAGAG-3'
Cxcr4 Forward	5'- TTTCAGCCAGCAGTTTCCTT-3'
Cxcr4 Reverse	5'- TCAGTGGCTGACCTCCTCTT-3'

CRISPR/Cas9 guide RNA sequences

SnoN exon1 Guide 1	5'-TGACCGACATTCATGCCAAT-3'
SnoN exon1 Guide 2	5'-TAGAGAAACACGGTTTCGCT-3'
SnoN exon1 Guide 3	5'-GCGAATGCATGACGAACGTC-3'
SnoN exon1 Guide 4	5'-CGGGTGTCCCTAGGTATTTT-3'

c-Ski exon1 Guide 1	5'-CATGAGCTCGCTGGGCGGCC-3'
c-Ski exon1 Guide 2	5'-GGCCGCTTTCTCGGCGCGCT-3'
c-Ski exon1 Guide 3	5'-CCGCTGCCTGGACGACGTGA-3'
c-Ski exon1 Guide 4	5'-TGCCAACAAGTACAAGCGGA-3'

Smad7 Guide 1	5'-TGCGCCCGGCGGCGAGGACG-3'
Smad7 Guide 2	5'-GCGACGGACGGCCGGGCTTA-3'
Smad7 Guide 3	5'-CGTCCTCGCCGCCGGGCGCA-3'
Smad7 Guide 4	5'-CGGGAAGATCAACCCCGAGC-3'